13 Production Issues of Acidic Petroleum Crude Oils

Christian Hurtevent, Guy Rousseau, Maurice Bourrel, and Benjamin Brocart

CONTENTS

13.1 INTRODUCTION

13.1.1 Acidic Oil Origin and Related Production Problems

Many oil fields recently discovered in deep offshore in Angola, Congo, and Nigeria produce oil with a high acid content. However, this observation is not limited to West Africa; some fields in the North Sea and in Venezuela have the same characteristics (Table 13.1).

Naphthenic acids in petroleum are considered to be a class of biological markers [1–3] closely linked to the degree of biodegradation of the fields. Naphthenic acids are predominantly found in immature, biodegraded, heavy crudes [4]. The alteration of petroleum by living microorganisms, which may occur, for example, when meteoric water infiltrates an accumulation [5], significantly increases the density of the crude and, at the same time, decreases the level of paraffinic components. It is highly probable, therefore, that acidic crudes contain low levels of paraffins and have higher densities than nonacidic crudes. The correlation is quite good for all wells on the same field or for all fields located in the same block (Table 13.2).

In oil and gas production, acidic crudes cause scale to form inside tubing or in surface installations. The scale is often a mixture of calcium soaps associated with other minerals such

TABLE 13.1
Total Acid Numbers (TANs) of Crudes from Different Fields

Crude	Country	TAN (mg KOH/g)
CAMELIA	Angola	1.90
DALIA 2	Angola	2.37
ORQUIDEA	Angola	3.73
MOHO	Congo	0.87
BILONDO	Congo	1.80
UKOT	Nigeria	1.01
AFIA	Nigeria	1.20
IME	Nigeria	2.08
ALBA	North Sea	1.83
CAPTAIN	North Sea	2.32
HEIDRUN	North Sea	2.60
LAGOTRECO	Venezuela	1.18
MEREY	Venezuela	1.24
LAGUNA	Venezuela	4.10

TABLE 13.2
Paraffin Level, API Degree, and TAN Values for Acidic Crudes from Angola Block 17

Crude	%Paraffin	°API	TAN (mg KOH/g)
CAMELIA	0.49	23.02	1.90
DALIA 3	1.33	23.68	1.37
TULIPA	1.61	24.14	1.11
LIRIO	3.47	32.38	0.54
GIRASSOL	5.34	30.60	0.38
CRAVO	5.90	32.88	0.35

as calcium carbonate, clays, iron carbonate, etc. Such type of scales have been found in several countries, for example:

- Nigeria, on the Afia field
- Indonesia, on the Attaka field
- Great Britain, on the Blake field
- Norway, on the Heidrun field
- Angola, on the Kuito field
- China, on the EDC field
- Cameroon, on the Kita and Asoma fields

It has been discovered only recently [6] that such calcium soap scale is composed primarily of the calcium salt of a tetra-acid ($M_W \sim 1230$). Identified by Statoil and named ARN, this acid is the main component of all the scale already analyzed.

In the case of the Kuito field in Angola, 135 tons of scale had to be removed mechanically from two separator strings, the cleaning operation took 1 month, incurring considerable expenses and production losses.

On the Heidrun field in Norway, before an appropriate inhibitor was formulated and injected, 500 kg of scale a day were generated in the separators. In 1985, when production started on Kita in Cameroon, 80 m^3 of scale comprising a mixture of napthenates and calcium carbonate had to be removed from the electric desalters.

Among the fields that have experienced problems due to the formation of calcium soap scale, most of them have a high total acid number (TAN) relative to their API degree (Figure 13.1).

This particular characteristic can also be found in the Usan reservoir in Nigeria. In this case, the high TAN relative to the API can be explained by the multiple hydrocarbon formation and migration phases in the reservoir. These migration and formation phases at the scale of reservoir geology can be explained simplistically as a mixture of several oils with different characteristics.

In reservoirs like Usan, biological tracers have also been found, indicating high biodegradation, whereas elsewhere, a high API degree and a large quantity of paraffins were recorded, indicating at the scale of reservoir geology that this reservoir contains at least two different hydrocarbons. Many types of crude producing calcium soap scale fit into the latter case.

Depending on the nature of the naphthenic acids present in the oils, the formation of stable emulsions, associated with the very strong surfactant capacity of the naphthenate group, may also be observed in the separators. These emulsions, which cause separation problems, usually generate discharge waters having a high hydrocarbon and naphthenate content. Here, the naphthenic acids

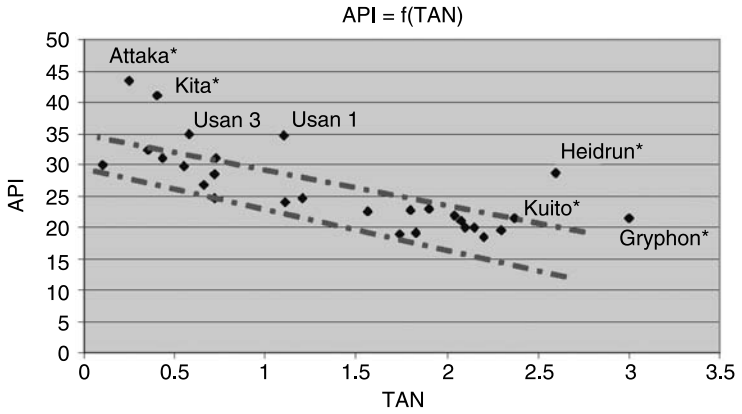

FIGURE 13.1 Relation between TAN and API for different fields. * These fields gave calcium soap scales.

responsible for such emulsions are not the ARN, responsible for scale, but rather monoacids with lower molecular weights (~200 to 400).

Refineries are concerned by the potential corrosivity of acid crudes at high temperatures. It is for this reason that these crudes are downgraded on the basis of their TAN value. The downgrade may be estimated using the following formula:

$$\text{Downgrade in \$/Bbls} = (\text{TAN} - 0.6)/2$$

where TAN is expressed in mg KOH/g.

13.1.2 Challenges Associated with Acidic Crudes

In the context of a new development project or assistance for an operator who is facing problems of the above type, the following points must be addressed.

13.1.2.1 Prediction of the Risks of Scale and/or Emulsion

For the producer, this essentially means being able to predict the risk of formation of emulsion and/or scale in the pipes or surface installations. The tools developed so far are insufficient and the models commercially available in this domain do not apply, since they imply a balance between the aqueous phase and the organic phase, and also since the parameters to be taken into account have not all been identified.

The acidity of a crude by itself is not a sufficient criterion; some weakly acidic oils in Cameroon or in Indonesia [7] may form stable emulsions while other highly acidic crudes can be treated with no problem. It is the actual structure of the naphthenic acids that may explain these differences in behaviors, whence the importance of characterizing the naphthenic acids of a crude.

Identifying the entire set of reactions that occur in each phase and at the water–oil contact, and characterizing the naphthenic acids, particularly their surfactant capacity, are the two first steps that allow us to model the balances and therefore to more accurately evaluate the potential risks associated with the treatment of acid oils.

Moreover, although it has been possible to identify the ARN in many deposits, it is still very difficult to identify this molecule in oils. Initial tests conducted by adding specific amounts of ARN to an oil showed that the methods of analysis described later on in this paper have a detection sensitivity of less than 50 ppm. This molecule is therefore present in oils at concentrations of a few ppm and must be concentrated (through deposit preparation, for example) to be identified. Recently, we have been able to find it in sludge prepared in our laboratory (unpublished result).

13.1.2.2 Prevention of Deposits and/or Emulsions

In some cases, like Kuito, modifying the separation process was sufficient to substantially decrease the mass of scale.

Some dispersants produce good results, especially with the Heidrun crude.

13.1.3 Theoretical Background on Calco-Carbonic and Naphthenic Equilibria

13.1.3.1 Calco-Carbonic Equilibrium

Reservoir waters are naturally saturated with carbon dioxide which produces carbonic acid, H_2CO_3. At bottom hole conditions, water is at equilibrium with the rock and the gas of the reservoir. On the other hand, during production, water is drained to the surface and undergoes significant pressure and temperature variations in the tubing, downstream from the choke at the well head, in the exchangers or in the separators.

The successive pressure drops lead to degassing of the carbon dioxide with an increase in the pH value of the produced water. This pH increase induces the formation and precipitation of calcium carbonate which has very low solubility, thereby generating undesirable deposits which plug the chokes or fill the separators. The chemical relation between carbon dioxide, pH value, and calcite solubility can be expressed as follows:

$$\mathbf{CO_2 + H_2O \Leftrightarrow HCO_3^- + H^+}$$

$$\mathbf{Ca^{2+} + HCO_3^- \Leftrightarrow CaCO_3 + H^+}$$

13.1.3.2 Naphthenate Equilibrium

The so-called "naphthenic acids" are mainly carboxylic acids with saturated cyclic structures, represented by a general formula $C_nH_{2n-z}O_2$, where n indicates the carbon number and z specifies a homologous series, from 0 for saturated acyclic acids to 8 in tetracyclic acids [8].

Naphthenic acids of low molecular weight contain alkylated cyclopentane carboxylic acids with smaller amounts of cyclohexane derivatives:

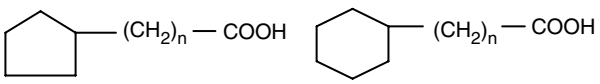

One thousand five hundred acids were identified in a single California crude [9] with boiling points ranging from 250 to 350 °C. They are fully soluble in organic solvents and fairly insoluble

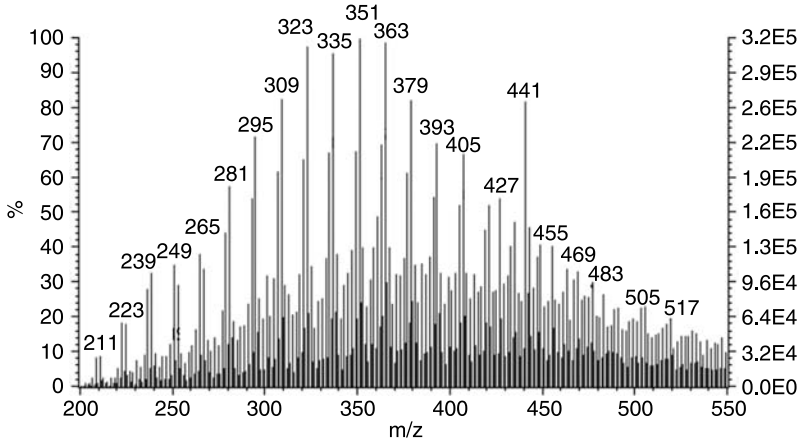

FIGURE 13.2 Dalia 3 acid characterization.

in water. Figure 13.2 shows the results of mass spectrometry analysis of the naphthenic acids extracted from Dalia 3 by anionic resin.

The naphthenic acids of the crude will follow acid–base equilibrium reactions in a multiphase system, which imply (1) acid partitioning between oil and water phases, characterized by a partition coefficient, and (2) acid dissociation, described by a dissociation constant (pKa). These phenomena are incorporated in a model presented in Section 13.4.

A number of studies have attempted to determine the pKa [10,11] of the various families of naphthenic acids – a complicated task in view of the number of different acids present in a given crude. However, this pKa value does not take into account the very low solubility of these organic acids in the water phase. At a given pH, the total amount of dissociated acids depends not only on the pKa value, but also on their partitioning coefficient. The higher the pH value, the heavier the naphthenates formed, even if the pKa values of light and heavy acids are close. Therefore, the potential capacity for a naphthenic acid to create stable emulsions depends on its partitioning coefficient, which may be correlated to its molecular weight. In a report published in 1969, Seifert and Howells state that the average molecular weights of interfacially active acids range from 300 to 400 [35].

The cations in reservoir water can react with $RCOO^-$ naphthenate groups to form salts, commonly named soaps, essentially sodium and calcium naphthenates, which dissolve in either water or oil, depending on their affinity for one phase or the other.

Sodium naphthenates having a low molecular weight tend to dissolve into the water phase. Calcium, as a divalent cation, is associated with two naphthenate groups, yielding lipophilic calcium naphthenates partitioning preferentially into the oil phase or adsorbing at the oil/water interface [12,13].

When the soap concentration exceeds the solubility, the precipitation of a solid deposit or in some cases the formation of an intermediate third phase at the interface between the oil and the water phases is observed. Sludge containing mainly sodium naphthenates has been observed on the Serang field [7] in Indonesia.

Contrary to field observations, in lab experiments we never observed solid deposits. We have only observed the formation of sludge of sodium and/or calcium naphthenates, possibly due to

the formation of mesophases [14–16]. Interestingly, ARN has been found at least in one case, in sludges formed from the Usan crude.

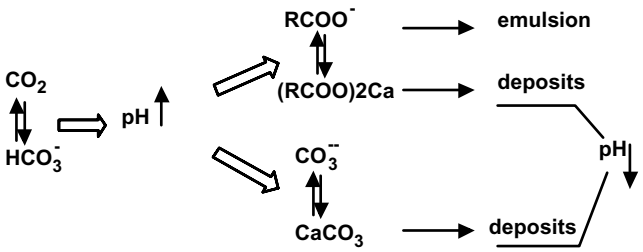

The release of CO_2 due to a shift in the calco-carbonic balance causes the pH value of the reservoir water to increase. This is followed by a competition between the formation of sodium or calcium naphthenate and the precipitation of calcium carbonate. The result is the potential formation of calcium carbonate deposit and/or emulsion stabilized by sodium/calcium naphthenates, and/or ARN deposits associated with a decrease in the pH value, if the water is not buffered by bicarbonate.

In the absence of bicarbonate, an increase in the pH value due to CO_2 degassing produces naphthenates and, at the same time, the dissociation of the naphthenic acids releases protons which act against the increase in pH, and thus impedes the formation of naphthenates. In the opposite case, naphthenates are produced as long as some bicarbonate is available to buffer the medium.

Thus, the species which mainly contribute to naphthenate formation are $RCOO^-$, Na^+, Ca^{2+}, and HCO_3^-.

From this, it may be assumed that the following criteria should be taken into account when predicting the formation of stable emulsion and/or scale in the processing of an acidic crude:

- For water, its pH value at process conditions and the level of bicarbonate and calcium content at reservoir conditions
- For oil, the amount of available naphthenic acids

Carbonates produce scale, whereas naphthenates can form emulsions at the water–oil contact, and ARN can form scale. None of the models on the market factor-in this potential competition in acidic crudes. As a result, the precipitable quantities of calcium carbonate are systematically overestimated.

13.1.4 Emulsion Stabilization by Naphthenates

The stability of water in crude oil emulsions is described in Section 13.3. The general conclusion of these tests is that the emulsion stability is strongly dependent on pH.

On a given oil field, the stabilization of emulsions by naphthenates depends on the capacity of naphthenic acids to form naphthenates at the lowest possible pH. Effectively, in the treatment of acidic oils, the pH increases throughout the entire process when the pressure decreases.

We have looked at the quantity of acid likely to react with the aqueous phase as a function of pH, for several crude oils. The measurements were carried out on a mixture of 90% oil and 10% water containing increasing quantities of caustic soda. The results are given as final pH, after the transfer of acids into the water as naphthenates, versus the quantity of naphthenates formed.

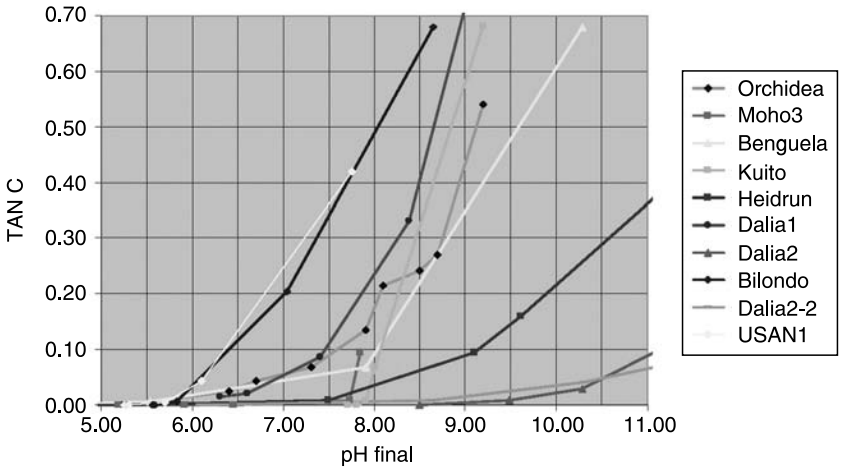

FIGURE 13.3 Naphthenate formation as a function of pH.

These naphthenates are expressed as the TAN (TANc) equivalent to the quantity of naphthenic acids that have come out of the oil (see Section 13.3 for more details).

The curves in Figure 13.3 show that some crude oils form naphthenates from pH as low as 6, whereas others only begin to form them at a pH value greater than 8 to 9. As naphthenates can be powerful surfactants, the risk of forming emulsions is especially greater whenever the transfer of acids occurs at a low pH.

In a petroleum installation, the gas associated with the produced oil generally contains a given proportion of CO_2. When the pressure decreases, CO_2 degassing promotes an increase in the pH value, simulated by soda addition in Figure 13.3. The formation of naphthenates will increase as the pressure in the installations decreases. One of the important ideas generated from this observation is that emulsion problems can be reduced if the water is separated from the oil at the highest possible pressure. As naphthenates are soluble in water, they will also have a strong tendency to carry oil into the water and therefore cause significant downgrading of the produced waters.

These naphthenates dissolved in the water are not included in the 30 to 40 ppm stated in the standards for determining hydrocarbon levels in produced waters. Effectively, naphthenates, being polar compounds, are retained by the silica generally used in methods for determining hydrocarbon levels. These compounds, which are almost nonexistent in water in a process occurring under pressure, may represent several hundreds of ppm when a process at atmospheric pressure is used. Though these compounds are not counted as hydrocarbons, the use of a process under pressure for oil/water separation is highly recommended for strictly environmental reasons. Certain regulations, onshore in particular, impose threshold values of total organic carbon (TOC). This property of crude oils concerns not only those crude oils qualified as acidic, but also all crude oils having a significant TAN. The same observations have been made on crude oils having a TAN of 0.3. Transfer of naphthenic acids from the oil phase as naphthenates in the water phase is described in Section 13.4 below, on modeling.

13.2 CHARACTERIZATION OF NAPHTHENIC ACIDS IN CRUDE OILS

The difference in behavior observed during the processing of acidic crudes mainly arises from the difference of the nature of the acids; which is why it is expected that the isolation and

characterization of naphthenic acids could be of prime importance for the prediction of the associated risks. The standard methods used to analyze naphthenic acids are discussed hereafter with a special interest to mass spectrometry.

13.2.1 Naphthenic Acids Quantification in Crude Oils

There are several methods for the determination of naphthenic acid content, which, unfortunately, yield different results.

13.2.1.1 ASTM Procedure for Total Acid Number

Assessment and predictability of corrosion by naphthenic acids are generally based on the determination of total acid number (TAN) and total sulfur in the crude oil [17]. Acid numbers are expressed numerically as mg KOH required to neutralize the acidity in 1 g of sample. However, the rules of thumb used in most refineries to predict corrosion based on TAN, sulfur species, based on previous experiences indicate a limited applicability of these characteristics since it has been discovered that crudes having a high TAN could be noncorrosive. Thus, high vacuum units, alloyed to deal only with sulfidation, have successfully processed feed stocks having a TAN of 4 mg KOH/g for more than 37 years [18]. More recent research has begun to highlight deficiencies in relying upon this method to quantify the oil acidity; ASTM D974 is a colorimetric titration method and has a reproducibility of 15%. ASTM D664 is a potentiometric titration method with reproducibility of 20% depending on the end point, type of oil, and titration mode. Inorganic acids, esters, phenolic compounds, salts, and additives such as inhibitors and detergents interfere with both methods. In fact, all compounds that react with potassium hydroxide (including hydrogen sulfide) are counted as acids; this is the case with calcium or iron naphthenates. Consequently, TAN is no longer regarded as such a reliable indicator of acidity [19].

13.2.1.2 FT-IR Spectroscopy

The measure of the absorbance at 1710 cm^{-1} by FT-IR spectroscopy is another method used to quantify specifically the acidity of crude oils [20]. An example of spectrum is shown in Figure 13.4.

Naphthenates can also be evaluated using the same method by quantification of the ester carbonyl band near 1600 cm^{-1}. The results are expressed respectively as neutralization and saponification values. The procedure requires calibration with known compounds in an oil representative of the samples to be analyzed.

We found a good correlation between the concentration of acids determined by FT-IR and TAN values: the higher the absorbance at 1710 cm^{-1}, the higher the TAN. This is illustrated in Figure 13.5 where the surface of the peak measured at the specified wavelength is plotted versus TAN for several crude oils. The FT-IR method is more reliable than TAN regarding the quantification of acidity, but is not usable for crudes having a low acidity.

In MOBIL analytical method 1463-89, acids are first separated from the crude oil sample using an amine bonded silica gel Sep Pak cartridge. Then the naphthenic acids are eluted from the cartridge with acetone and methanol and finally analyzed by IR spectroscopy.

Unfortunately, the instrument is calibrated with a purchased mixture of crude naphthenic acids, which are likely not to have the same composition and molecular weight as the sample. Thus, the weight percent can be used for comparison purpose only.

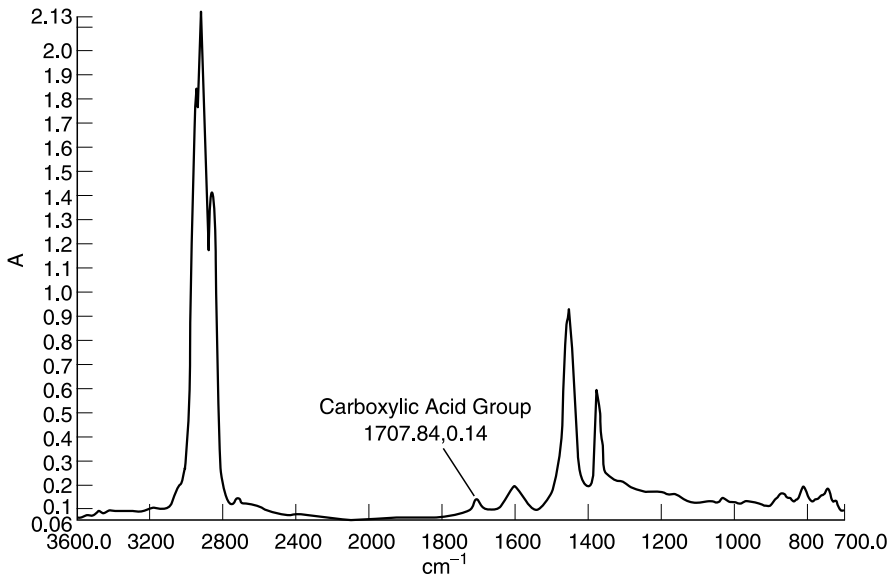

FIGURE 13.4 FT-IR spectrum of crude oil.

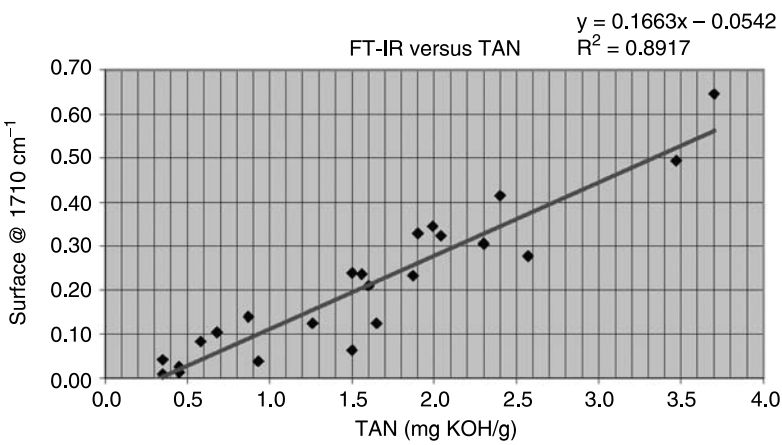

FIGURE 13.5 Comparison between TAN values and acidity quantified by FT-IR.

Another variation of the chromatographic method is the naphthenic acid number (NAN) or naphthenic acid titration (NAT) whereby the sample is extracted by chromatography and then titrated per ASTM D664 [19].

13.2.1.3 Gas Chromatography

Naphthenic acids comprise a highly complex mixture containing hundreds of compounds that are impossible to separate into individual components, even by high resolution chromatography.

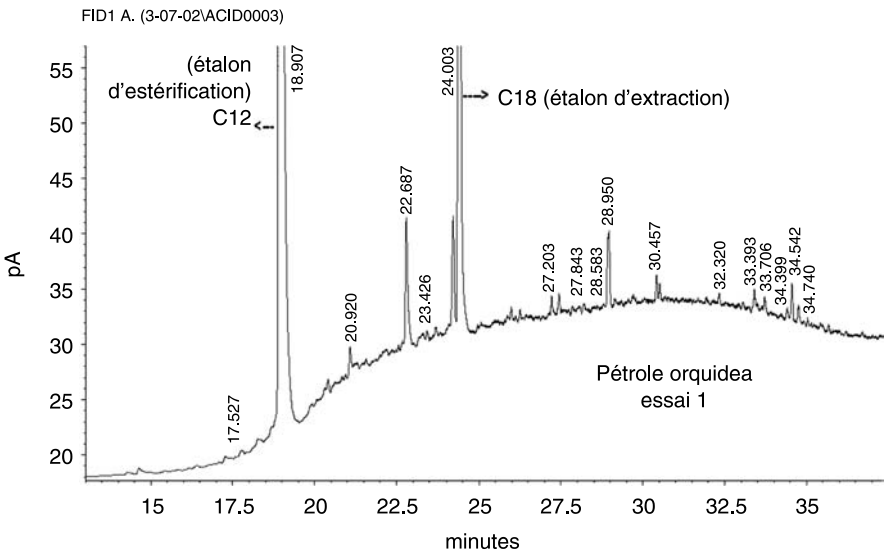

FIGURE 13.6 GC spectrum of esterified naphthenic acids after extraction from Orquidea crude oil.

The most described technique is based on a liquid–liquid or solid–liquid extraction of naphthenic acids from the crude oil sample followed by the derivatization of the isolated fractions as methyl esters [21,22]. Acids are analyzed by gas chromatography with a cold on-column injector and a flame ionization detector using HT-5 capillary column.

The percentage of acids in the crude is quantified by measuring the total GC-FID chromatogram areas above the baseline of the blank (hexane) analysis through the internal standard (C12), assuming a response factor of 1. Chromatograms of the extracted and esterified acids from crudes present a strong background noise, as illustrated in Figure 13.6. The peaks seen at approximately 19 and 25 min correspond, respectively, to the lauric and octadecanoic acids used as internal and extraction standards [9].

13.2.2 Naphthenic Acid Extraction from Crude Oil

One of the key points in naphthenic acid characterization is to use the suitable procedure to extract all the acids from the crude. The different methods are grouped into the categories of: solid–liquid extraction, liquid–liquid extraction, and chromatography.

Acid-IER (ion exchange resin) is the preferred method; carboxylic acids in the crude are selectively extracted by an alkaline resin. They are adsorbed onto the resin as naphthenates $RCOO^-$ that are later desorbed during the regeneration of the resin by sodium hydroxide. The acids are recovered after acidification and dichloromethane back-extraction.

AMBERLYST® IRA 900 or QAE Sephadex A-25, strong negative ion exchangers, are both suitable for such an extraction. The adsorption of the acids on the resin can be done either in a batch process or by flowing the crude through a column. The amount of needed resin roughly corresponds to 10 equivalents of base per equivalent of acid determined by TAN measurement.

The extraction yield can be very different depending on the used procedure or on the nature of the crude. Results from 60% to 90% have been found with the same crude, just by running the extraction at a different temperature or for a longer time. A suitable procedure has been optimized

and is described in an SPE paper [23]. According to STATOIL, it would allow recovery of up to 97% of the acids from a Norwegian crude oil sample.

13.2.3 Naphthenic Acid Characterization

Research has shown that the corrosivity of naphthenic acids is related to their molecular mass [24–26] and that the "total acid number" (TAN), traditionally used as an indicator of the naphthenic acid content of an oil, is not as reliable as first believed. With regards to these concerns, mass spectrometry has been increasingly applied to the investigation of the naphthenic acid content of crude oils.

13.2.3.1 Determination of Naphthenic Acids by Mass Spectrometry

The techniques used have included: gas chromatography mass spectrometry (GC-MS) [27], electron ionization (EI) [27], liquid secondary ion mass spectrometry (LSIMS) [28], chemical ionization (CI) [29], atmospheric pressure chemical ionization (APCI) [29], and, recently, electrospray ionization (ESI) [30–32]. Electrospray ionization is the ionization technique which holds the greatest promise for the successful characterization of naphthenic acids in crude oil samples.

A variation of ESI that is more attractive for this purpose is nano electrospray ionization, also known as "nanospray" [33]. Nanospray entails the use of a fine glass needle, coated in a conductive layer such as gold and/or palladium, into which the sample is loaded. No pumping is required and the ions are formed and extracted through the use of a strong electrical field alone.

Fast atom bombardment mass spectroscopy (FAB-MS) [2] uses the negative ion detection mode; it detects the $(M-1)^-$ ion in carboxylic acids, including high molecular species with no fragmentation. FAB-MS determines the molecular weight distribution of the naphthenic acids extracted from the oil. Component information, based on carbon number and acid group type distributions, is obtained clearly from the FAB spectrum. The results show that this group type distribution provides a fingerprint that can be a valuable tool to predict the risks associated with crude oils processing.

FAB-MS gives all the masses of the acids extracted from the crude ranging from 150 to 650, centered on 350. However, acids having the same nominal molecular weights but different formulas, such as $C_{14}H_{26}O_2$ and $C_{15}H_{14}O_2$, are not completely resolved under the operating instrument resolution. Typical LC/MS ESI negative mode spectra are presented in Figures 13.7 and 13.8.

13.2.3.2 Determination of Naphthenate Deposits by Mass Spectrometry

Recently, the STATOIL Company has identified the dominating naphthenic acid in naphthenate deposits [6]; it would be a 4-protic acid with a molecular weight in the range of 1227 to 1235 g/mol, called ARN, acid. The presence of that acid would be a universal characteristic of oilfield naphthenate deposits. It is not possible by LC-MS to determine the detailed structure of ARN, but its formula would correspond to $C_{80}H_{142}O_8$. This acid has been detected by FTMS and LC-MS in naphthenate deposits from West Africa dissolved in a blend of one aromatic solvent and acetic acid (Figure 13.9).

The first part of the mass spectrum is representative of the naphthenic acids commonly found in acidic crudes, but one can see a peak with the highest relative intensity at $m/z' = 1230$ corresponding to the acids specific of deposits. The presence of a doubly charged ion at $m/z' = 614.5$ confirms the fact that naphthenate deposits are multiacids. The 4-protic acid claimed by STATOIL could be seen by high resolution MS as it would become possible to see other charged

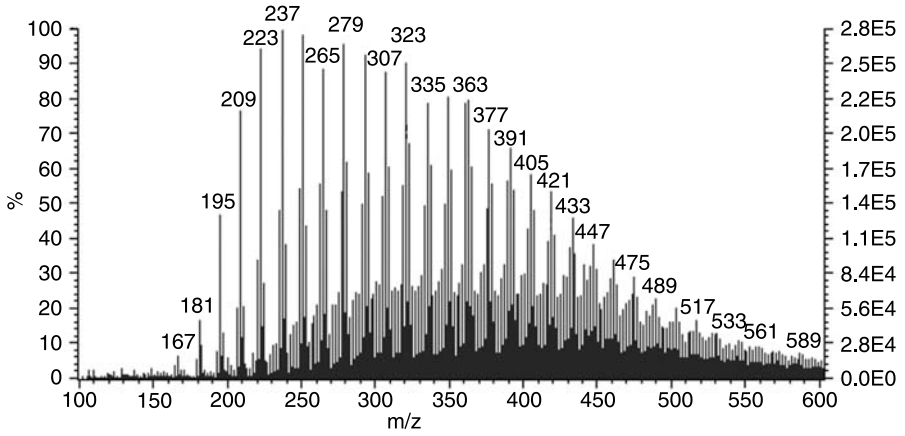

FIGURE 13.7 LC/MS spectrum of Orquidea crude oil from West Africa.

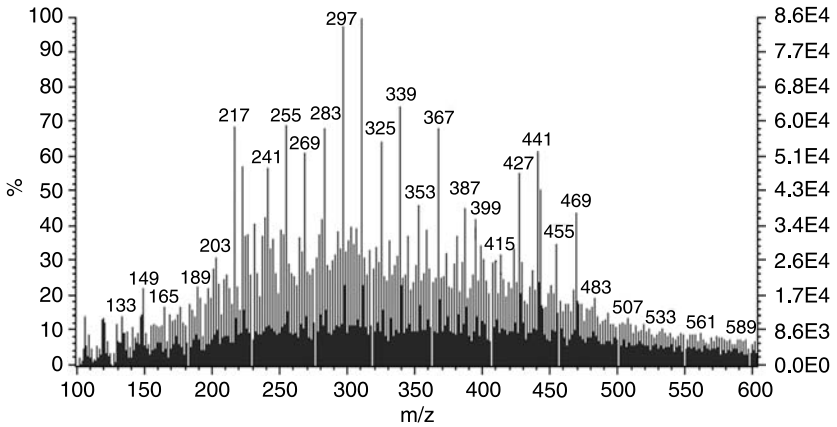

FIGURE 13.8 LC/MS spectrum of Dalia 2 crude oil from West Africa.

ions at m/z′ = 410 and m/z′ = 307.5. However, this new discovery demonstrates the great interest of mass spectrometry to predict a potential risk of naphthenate deposit.

13.2.3.3 Characterization of Naphthenic Acids by FTMS

The most interesting analytical methods for the characterization of naphthenic acids in crude oils are based on the extraction of the acids followed by soft ionization mass spectrometry techniques.

The composite mass spectrum provides an envelope that follows the molecular weight distribution of the mixture. The naphthenic homologs are represented by a general formula $C_nH2_{n-z}O_2$, where n indicates the carbon number and z specifies a homologous series. z is equal to 0 for saturated aliphatic carboxylic acids; it increases by 2 with the increase of hydrogen deficiency resulting from the formation of rings or double bonds in the molecule. Some typical naphthenic structures, where z = 2 to 8, are shown in Figure 13.10.

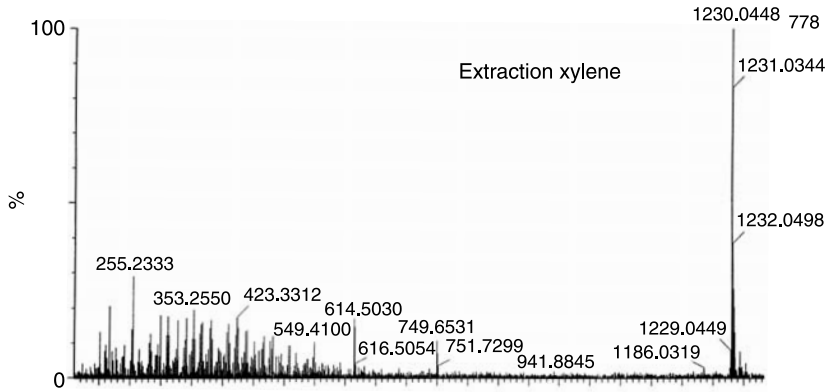

FIGURE 13.9 LC/MS spectrum of naphthenic acids extracted from a calcium naphthenate deposit from West Africa.

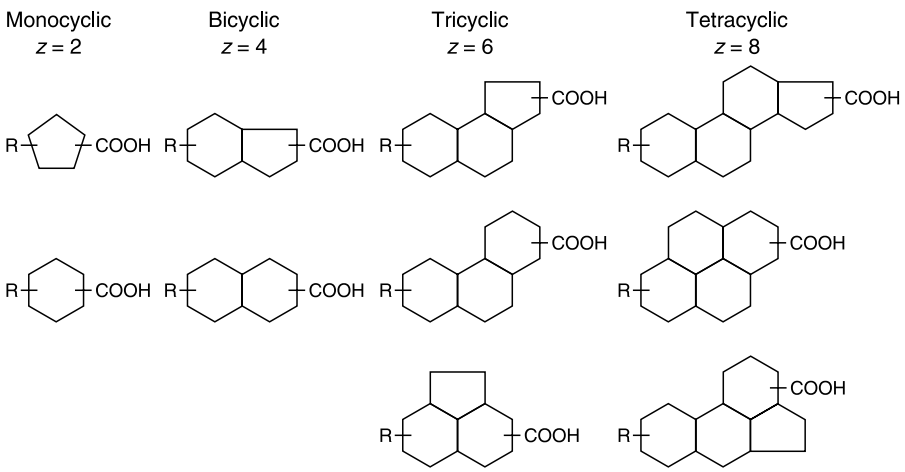

FIGURE 13.10 Typical naphthenic acid structures, where R = alkyl.

A number of isomers may be present in the same homologous z series but cannot be distinguished by standard methods on the basis of the observed $(M - 1)^-$ ions. For example, regarding the hydrogen deficiency corresponding to z = 8, the structure that fits with the molecular weight can be either aliphatic or even aromatic (Figure 13.11).

Some isomers can be identified by using Fourier transform ion cyclotron resonance mass spectrometry (FT-ICR MS or FTMS) technique, regarding its inherent high mass accuracy and high resolution [34]. A 9.4 T FT-ICR mass spectrometer was used in order to illustrate the advantage of routine high resolution, permitting the distinction to be made between nominally isobaric acid species. Nanospray has been selected as the ionization technique to combine the advantages of reduced sample fragmentation, the inherent sensitivity of nanospray, and minimization of the risks of instrument contamination.

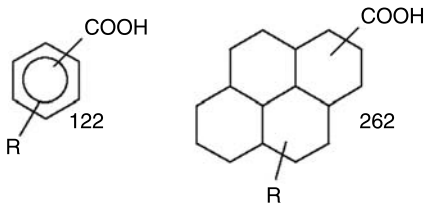

FIGURE 13.11 Possible naphthenic acid structures corresponding to a deficiency of eight hydrogen atoms.

Ten crude oil samples were analyzed using the negative-ion mode to determine the presence of different naphthenic acid species. Spectra obtained in the positive-ion mode contained approximately three times the number of signals, as species other than the acids could be observed, and were thus more complex with regard to the data analysis stage.

Once the spectrum had been acquired, the resulting data processed with XMASS was imported to a spread sheet and sorted into corresponding z homologs and carbon contents, comparing the theoretical m/z ratio with the experimental value. Finally, graphs of the absolute intensities were plotted as a function of carbon content for each of the z homologs.

FTMS gives the exact mass of the extracted acids up to 8 decimals for molecular weights ranging from 300 to 650, centered on 450. Doublets were observed which revealed the presence of naphthenic acids with a high degree of hydrogen deficiency. Such signals would not be observable when using instruments such as quadrupoles and some time-of-flight instruments, which are frequently used for routine analyses. Eighteen families of acids could be identified, including diacids; however, it is not yet possible to determine whether aromatic rings are present simply from the empirical formula. Examples of FTMS spectrum and subsequent analysis of BILONDO crude from West Africa are shown in Figures 13.12 and 13.13.

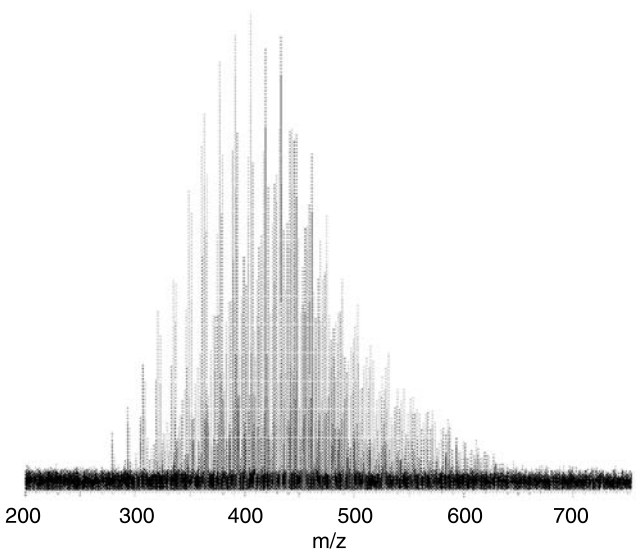

FIGURE 13.12 FTMS spectrum of BILONDO crude.

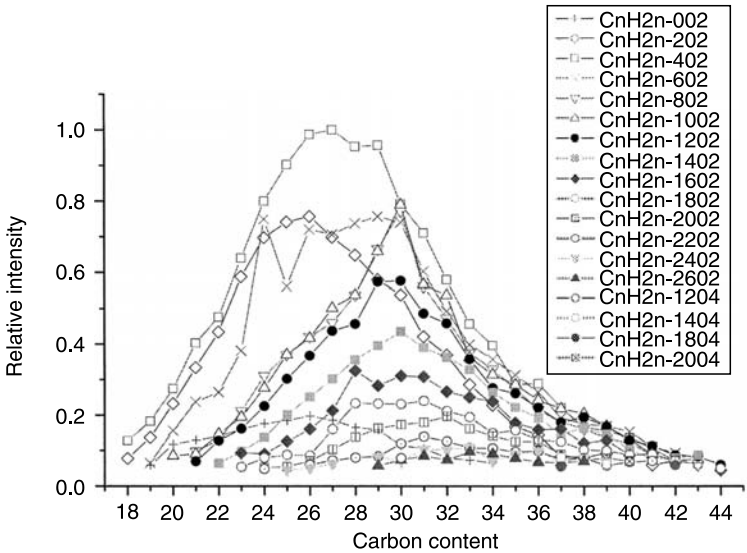

FIGURE 13.13 Distribution of naphthenic acids extracted from BILONDO crude and analyzed by FTMS.

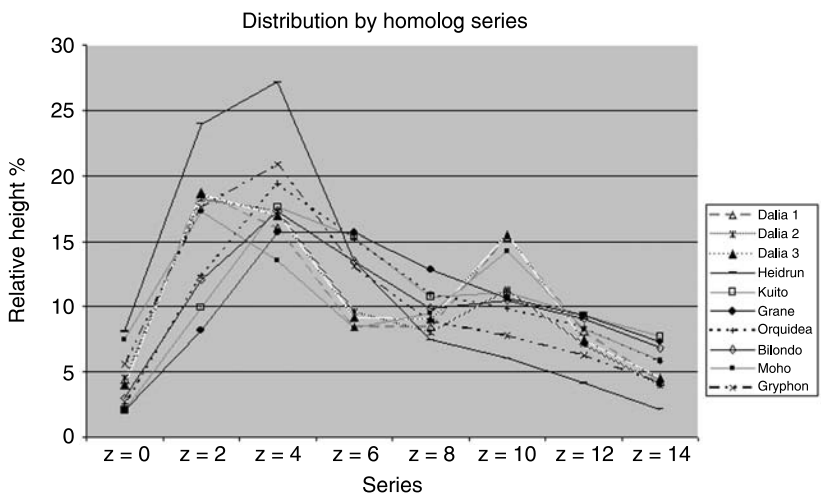

FIGURE 13.14 Comparative FTMS distribution of acids extracted from 10 crude oils.

The comparative FTMS distribution by homolog series of the naphthenic acids extracted from ten different crude oils is illustrated in Figure 13.14 for the first homolog series. From the results, we have been able to determine the average molecular weight of the extracted acids and observe significant differences: for instance, an average molecular weight of 380 for HEIDRUN crude, 440 for DALIA crudes, and 490 for ORQUIDEA crude. Seifert and co-workers claimed that the number average molecular weights of the interfacially active acids range from 300 to 400 [35].

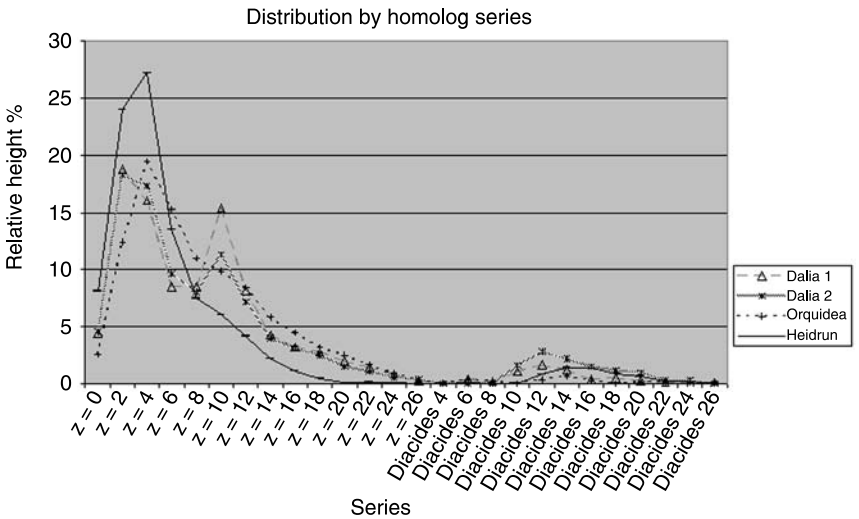

FIGURE 13.15 Distribution of the naphthenic acids determined by FTMS on acid extracted from various crude oils.

Regarding the distribution of the acids, we observed significant differences; all comparative data are given in Table 13.3. They are highlighted in Figure 13.15 for HEIDRUN, DALIA, and ORQUIDEA crudes, as they are deeply investigated in Section 13.3. HEIDRUN crude, known to form naphthenate deposits, has the highest amount of acids from z series 0, 2, and 4. DALIA 1 crude has the highest level of acids from z series 10 whereas DALIA 2 showed the highest level of diacides.

It is not possible at this stage to find the connection between naphthenic acid distribution and the risks associated with crude oils processing; however, by providing information about the composition and range of naphthenic acids present in a crude oil, information is obtained which can be used as a fingerprint that would identify a particular oil sample and link it to a particular oil field. On top of that, MS-MS technique associated with FTMS could be useful to identify aromatics, as well as to determine the nature of ARN responsible for naphthenate deposits.

13.3 PHYSICO-CHEMICAL BEHAVIOR OF ACIDIC CRUDE OILS

13.3.1 Materials and Experimental Techniques

A number of acidic crude oils have been studied, most of them coming from the deep off-shore fields of block 17 operated by Total in Angola. We present here first the results obtained with three crudes representative of the variety of behaviors observed with acidic crude oils [36,37]. Their characteristics are given in Table 13.4. The TAN has been measured according to ASTM D664 for the crudes and their cuts. The distribution of the acid species among the various cuts is different from one crude to another: Dalia 1 acids are concentrated in the 150 to 230 cut, contrary to Orquidea. Dalia 2 exhibits a high acid content in the heaviest cut (550+).

Emulsions were prepared by mixing brine (20 ml) and crude oil (180 ml) with a whisking system in a 500 ml beaker. The rate and application time of the whisk were chosen according to the nature of the oil in order to obtain about 80% of decanted water after 8 h storage at 40 °C

TABLE 13.3
Distribution of Naphthenic Acids Determined by FTMS for Various Crude Oils

Series	Crude B (RH %)	Crude D1 (RH %)	Crude D2 (RH %)	Crude D3 (RH %)	Crude Ga (RH %)	Crude Gy (RH %)	Crude H (RH %)	Crude K (RH %)	Crude M (RH %)	Crude O (RH %)
$Z = 0$	3.0	4.4	4.5	4.0	2.1	5.6	8.1	2.1	7.5	2.5
$Z = 2$	12.1	18.7	18.2	18.6	8.2	17.6	24.0	10.0	17.3	12.4
$Z = 4$	17.3	16.0	17.3	17.0	15.7	20.9	27.2	17.6	13.6	19.4
$Z = 6$	13.5	8.5	9.6	9.2	15.6	13.1	13.5	15.3	8.4	15.3
$Z = 8$	9.9	8.5	8.1	9.1	12.9	8.9	7.5	10.8	9.5	11.0
$Z = 10$	10.5	15.4	11.3	15.5	10.7	7.8	6.0	11.1	14.3	9.9
$Z = 12$	9.1	8.2	7.1	7.4	9.3	6.3	4.1	9.3	8.3	8.4
$Z = 14$	6.8	4.3	4.0	4.5	7.3	4.2	2.2	7.7	5.9	5.8
$Z = 16$	5.3	3.2	3.1	3.6	5.3	2.9	1.1	5.4	4.4	4.5
$Z = 18$	4.1	2.8	2.5	2.5	4.0	2.2	0.5	3.9	3.2	3.2
$Z = 20$	2.9	2.0	1.5	1.7	3.1	2.0	0.1	2.5	1.9	2.5
$Z = 22$	2.1	1.4	1.1	1.1	2.4	1.1	0.1	1.5	1.7	1.7
$Z = 24$	1.7	0.8	0.5	1.0	1.9	0.7	0.0	1.2	1.5	0.9
$Z = 26$	1.1	0.2	0.3	0.1	1.5	0.3	0.0	0.5	1.0	0.3
Diacides 4	0.0	0.0	0.0	0.2	0.0	1.7	0.0	0.0	0.0	0.0
Diacides 6	0.0	0.4	0.0	0.7	0.0	2.4	0.1	0.0	0.0	0.3
Diacides 8	0.0	0.2	0.0	0.6	0.0	0.7	0.0	0.0	0.1	0.2
Diacides 10	0.0	1.0	1.6	0.8	0.0	0.5	0.0	0.0	0.5	0.0
Diacides 12	0.1	1.6	2.8	1.7	0.0	0.5	0.8	0.0	0.7	0.3
Diacides 14	0.2	1.2	2.2	0.3	0.0	0.5	1.4	0.3	0.0	0.7
Diacides 16	0.1	0.3	1.5	0.2	0.0	0.1	1.3	0.3	0.1	0.3
Diacides 18	0.2	0.5	1.1	0.0	0.0	0.1	0.9	0.3	0.1	0.0
Diacides 20	0.1	0.3	1.0	0.1	0.0	0.0	0.7	0.1	0.0	0.1
Diacides 22	0.0	0.1	0.3	0.0	0.0	0.1	0.3	0.0	0.1	0.1
Diacides 24	0.0	0.0	0.3	0.0	0.0	0.0	0.2	0.0	0.0	0.1
Diacides 26	0.0	0.1	0.0	0.0	0.0	0.0	0.0	0.0	0.0	0.0

RH = Relative Height

TABLE 13.4
Distribution of the Total Acid Number (TAN) Within the Different Crude Cuts

TAN (mg KOH/g)	DALIA 1	DALIA 2	ORQUI
Crude	1.4	2.5	3.4
150 to 230 cut	1.11	0.43	0.13
230 to 350 cut	2.28	2.70	3.73
350 to 400 cut	1.62	2.64	7.39
400 to 550 cut	0.35	0.58	1.25
550+ cut	0.40	1.05	0.20

for the least stable system (deionized water at pH = 5.5): 500 rpm during 10 s for Dalia 1 and Orquidea, 750 rpm during 30 s for Dalia 2. Before whisking, water was added according to the following procedure: aqueous solutions at given pH were prepared by adding solid NaOH to 200 ml of distilled water. 10 ml was poured in the 500 ml beaker. 180 ml of crude oil was then added and finally 10 ml of brine prepared by adding NaCl or $CaCl_2$ to distilled water. Amounts of NaOH, $CaCl_2$, and NaCl were calculated in order to reach the targeted pH value and sodium and/or calcium concentration for a water volume of 20 ml. Such a method was performed in order to prevent any precipitation by direct contact of OH^- with calcium chloride. The same procedure was carried out even in the absence of calcium chloride.

The 200 ml volume was then divided in two 100 ml bottle testers (ASTM D96) placed in a controlled temperature bath at 40 °C. The percentage of decanted water was followed over time. After 3 days, when decantation was too slow, phase separation was forced by centrifugation. On decanted water samples, pH was measured (pH_f), and found different from initial pH (pH_i). Surface tension measurements were performed on recovered water samples as a function of time with a drop tensiometer (IT Concept). Surface tensions at 4 min are reported. Similar experiments have been carried out on model systems, where the oil is n-heptane and the organic acids are the octanoic acid from Aldrich and naphthenic acid from Fluka (a mixture of average molecular weight = 230).

13.3.2 Results and Discussion: Crude Oils

The stability of water in crude oil emulsion was studied first as a function of pH. Figure 13.16 typically shows the fraction of non-separated water of Dalia 1 emulsions as a function of time. For each system, the initial (pH_i) and final pH (pH_f) are indicated.

Various systems are then compared by plotting the percentage of non-decanted water after 48 h against the final pH. Due to the consumption of NaOH by the organic acids of the crude, pH_f is generally lower than pH_i. We have reported in Figure 13.17 the evolution of pH_f as a function of pH_i for the three presented crudes. It is interesting to observe that pH_f varies only slightly over a wide range of initial pH_i, that is, over a wide range of NaOH concentration, and then increases for the highest pH_i. This behavior will be discussed at the light of the results obtained on model systems (Section 13.4.2). It is interesting also to notice that, for Dalia 1 and Dalia 2, the equilibrium pH is higher than the initial pH for $pH_i = 5.3$. This surprising result will be explained later in the theoretical section (Section 13.4.2). It is attributed to the presence of sodium and/or calcium naphthenates in the oil phase prior to contact with the aqueous phase. Dalia 2, especially, is known to contain around 150 ppm of calcium.

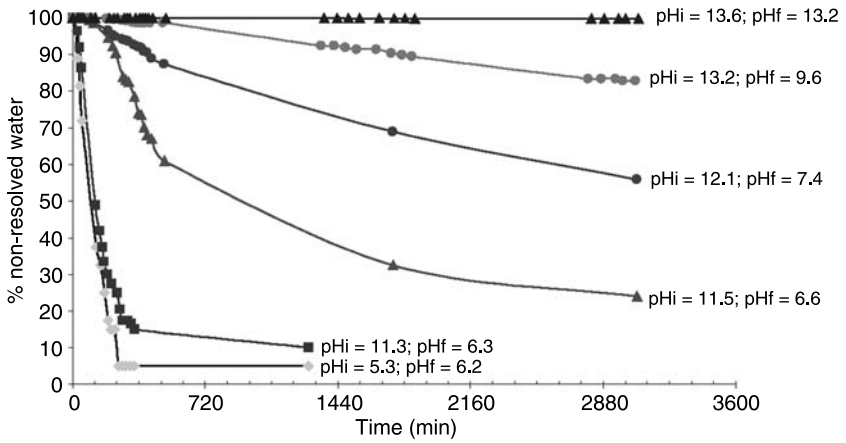

FIGURE 13.16 Stability of Dalia 1 crude emulsions.

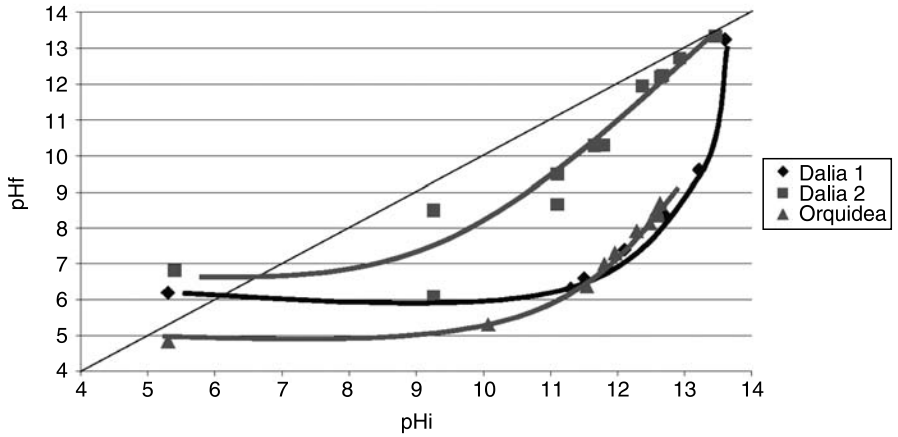

FIGURE 13.17 Equilibrium pH (pH_f) versus initial pH (pH_i) of water (10%) contacted with three different crudes (90%).

From pH_i and pH_f values, the amount of OH^- consumed has been calculated and expressed in TAN units: TAN_C. The ratio TAN_C/TAN represents the fraction of naphthenic acid originally present in the crude which have been neutralized by OH^- during emulsification.

13.3.2.1 Dalia 1 Results

The evolution of TAN_C/TAN with the final pH_f is reported in Figure 13.18 for the Dalia 1 crude. It increases progressively from $pH_f = 6.2$ to $pH_f = 13.2$. That is, at this pH, all the acids are neutralized by NaOH.

In a complementary way of evaluating the fraction of naphthenic acids neutralized by the base in each bottle test, it is interesting to calculate the fraction of the base introduced in the

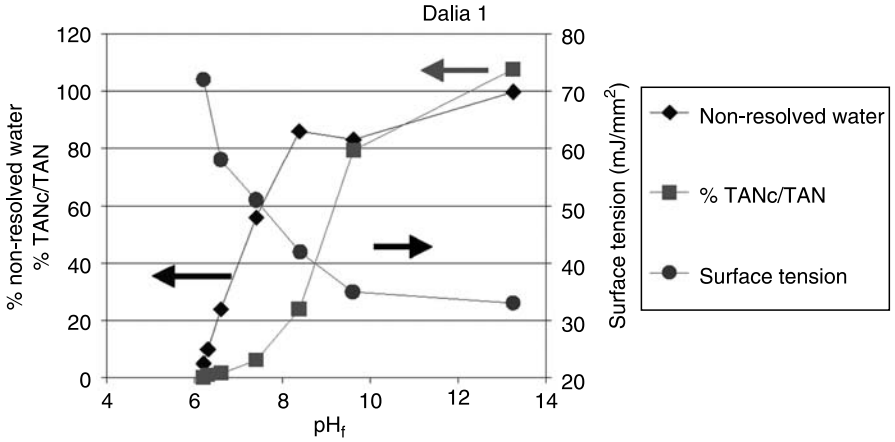

FIGURE 13.18 Dalia 1: emulsion stability, fraction of consumed TAN, and surface tension of the separated aqueous phase as a function of final pH.

system which has been consumed by the naphthenic acid. Similarly as above, the initial NaOH concentration has been expressed in TAN units = TAN_o, for "TAN offered." TAN_C/TAN_o is thus the fraction of initial NaOH neutralized by the naphthenic acid. In the present case of Dalia 1, all the base is consumed until $pH_f \sim 9.8$. Then, NaOH is in excess with respect to the naphthenic acid content, which explains the increase in pH_f.

Figure 13.18 also displays the surface tension of the decanted water as a function of the final pH. The value of the surface tension is linked to the presence of surface active species: a decrease in surface tension reveals an increase in concentration of surface active molecules in water. At $pH_f = 6.2$, the surface tension of the separated aqueous phase is 71 mN/m, i.e., very close to that of pure water: in the present case, no surface active species of the crude dissolve in the water. The undissociated naphthenic acids, which are known to display surface activity [38,39], do not partition into the water phase, as seen also from the pH_f value, despite the elevated TAN value of the lightest cut of the Dalia 1 crude (Table 13.4). Conversely, the basic species (sodium or calcium naphthenates?) which partition into water at this pH do not exhibit any surface activity. When pH_f increases, the water surface tension decreases markedly, indicating an increased partitioning of the naphthenic acids into water, more specifically of their salts. At the same time, the emulsion becomes more and more stable, accompanying the increase in TAN_C/TAN, which demonstrates further the surfactant character of the salts of the Dalia 1 naphthenic acids.

13.3.2.2 Orquidea Results

For Orquidea (Figure 13.19), although the same general features as for Dalia 1 are displayed, significant quantitative differences are observed. TAN_C/TAN, contrary to Dalia 1, varies only slightly when pH_f increases up to 8.5 roughly. Beyond that value, a sharp raise is observed, but, at $pH_f = 9.2$, only 25% of the naphthenic acids initially present in the crude have been neutralized. (At that point, TAN_C/TAN_o indicates that all the NaOH introduced in the system has been consumed.)

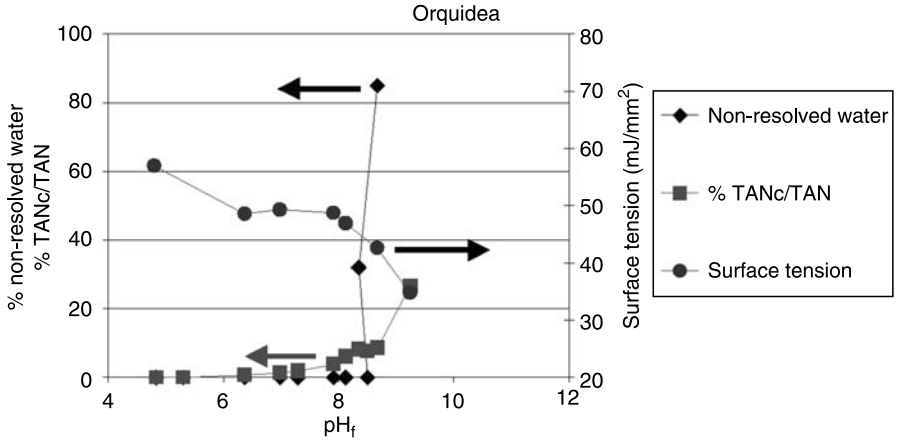

FIGURE 13.19 Orquidea: emulsion stability, fraction of consumed TAN, and surface tension of the separated aqueous phase as a function of final pH.

The surface tension of the extracted water phase is only 60 mN/m at $pH_f = 6.2$, which shows that some surface active species already partition into water at this low pH. Upon increasing pH_f to 8.5, roughly, the surface tension decreases only slightly, although the value of TAN_C/TAN_o indicates that all the base introduced in the system is neutralized by the crude. This suggests that the organic acids involved for $pH_f < 8.5$ are not highly active at the water surface. For $pH_f > 8.5$, the surface tension of water decreases significantly, indicating an increase of the partitioning of more surface active species.

Similarly, the emulsion stability curve exhibits an abrupt transition around $pH_f = 8.5$, where the emulsions become very stable. This is consistent with the transitions observed on TAN_C/TAN and on water surface tension, supporting the idea that two main types of naphthenic acids are present in the Orquidea crude: the first ones, likely of very low molecular weight, are soluble in water and display low surface activity, at least as regards the stabilization of water-in-oil emulsions. It is known from literature that the pK_a of such compounds is low, on the order of 4.7, which means that at $pH_f \sim 6.2$, there is a significant proportion of dissociated species. The other type of naphthenic acids, likely of higher molecular weight, displays the expected surface activity and strongly stabilizes the water-in-oil emulsion.

When looking at the distribution of TAN values among the various cuts (Table 13.4), Orquidea has clearly a stronger acidity in the heavier cuts compared to Dalia 1, which is coherent with the above interpretation. Regarding the light cut (150 to 230) it is, however, less obvious to correlate its TAN value to the observed phase behavior, unless it is speculated that organic acids might be present in even higher cut.

13.3.2.3 Dalia 2 Results

The results are reported in Figure 13.20. Again, as for Orquidea, TAN_C/TAN remains small when pH_f increases, but up to much higher pH_f value: 12 compared to 8.5 for Orquidea. Then a sharp increase is observed but again, at $pH_f = 13.3$, only 22% of the naphthenic acids of the crude are neutralized, although the calculation of TAN_C/TAN_o reveals that, at that point, 75% of the base is still available. This raises the question of the quality of the contact of the naphthenic acids of

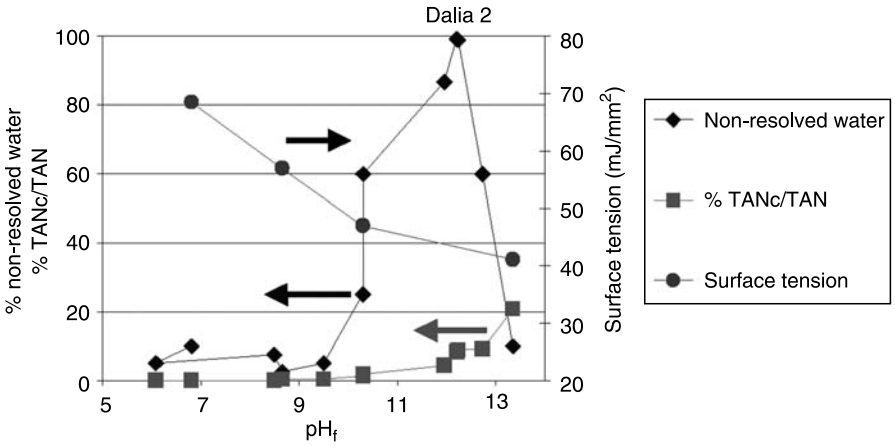

FIGURE 13.20 Dalia 2: emulsion stability, fraction of consumed TAN, and surface tension of the separated aqueous phase as a function of final pH.

the crude with the aqueous base, and thus the question of the initial agitation of the system. The experiment has thus been repeated, with a vigorous initial mixing of the fluids. The result should be approximately the same, indicating that some likely heavy naphthenic acids do not participate in the acid–base equilibrium under the conditions of the experiment (although they are counted in the TAN measurement, i.e., in the presence of methanol).

The surface tension of the aqueous phase starts, at $pH_f = 6.8$, with a value close to that of pure water (72 mN/m), as for Dalia 1, but then exhibits a more progressive decrease when pHf increases. Contrary to the previous cases of Dalia 1 and Orquidea, this strong increase in emulsion stability does not coincide with a large increase in naphthenate formation, as seen from TAN_C/TAN: the neutralization of only roughly 2% of the naphthenic acids is sufficient to produce a very stable emulsion, indicating likely that the naphthenates produced in these conditions ($pH_f \sim 10.2$) are particularly well adapted to Dalia crude (water-in-oil) emulsification. Above $pH_f = 10.2$, around $pH_f = 12$, three very stable emulsions are obtained, presenting a particular behavior: after some phase separation was achieved, a gel-like phase was observed at the water–oil interface.

At that point, it is important to mention that around 150 ppm calcium are present in the Dalia 2 crude. The calcium salts of long chain carboxylic acids are known to be highly hydrophobic and water insoluble, forming colloidal precipitates, or liquid crystal mesophases, or oil soluble complexes. This is further discussed below. In the present case, it is believed that the observed gel-like phase is due to the structure of calcium naphthenates, which, by adsorption at the water–oil interface, could also be responsible for the high emulsion stability of the three systems at $pH_f \sim 12$. Such compounds may form at lower pH_f, such as $pH_f = 10.2$, but in much smaller concentrations so that gel-like phases are not visible, but, because of their high hydrophobicity, they may be at the origin of the strong increase in emulsion stability observed at that pH_f.

Surface tension measurements performed on the centrifuged water from the very stable systems obtained at $pH_f = 12$ could not give reliable results: after a few seconds, some particles appeared at the water–air interface, modified the shape of the drop, thus confirming the presence of a third phase. Beyond $pH_f = 12.5$, it was again possible to measure properly the surface

tension of the decanted water, suggesting that the deposit does not form any more. At $pH_f > 12.5$, unstable emulsions are again obtained while the gel-like phase is no more observed. At such high pH, calcium hydroxide is no longer water soluble and likely precipitates, removing the calcium out of the system. The surface tension measured at $pH_f = 12.7$ and 13.3 are close to those measured before the strong stabilization regime. In view also of the continuity of the TAN_C/TAN curve (Figure 13.20), this suggests that the strong stabilization regime is essentially due to the presence of calcium naphthenate salts.

The three examples presented above illustrate the variety of behaviors encountered in the production of acidic crude oils. As a general trend, the increase in naphthenate formation (TAN_C/TAN) parallels a significant decrease in surface tension of the aqueous phase of the systems, indicating an increased concentration of surface active naphthenates in water.

This phenomenon does not, however, correlate necessarily with the stabilization of water-in-oil emulsions: the presence of calcium ions, or more generally of multivalent cations, may affect the phase behavior and produce coarse emulsions or even gel-like phases. These features are hardly predictable only from knowledge of the TAN distribution among the various cuts of the crude.

From a practical standpoint, the preparation of a series of bottle tests at various pH values according to the procedure presented above seems to be relevant for evaluating the potential risk of coarse emulsion or gel formation of a given crude upon pH increase. From this point of view, the Dalia 1 crude, which exhibits, under the conditions of the experiments, emulsion formation at the lowest pH, seems to be the most "dangerous" crude among the three investigated. It is interesting that it displays the lowest TAN. Indeed, the presence of multivalent cations is of paramount importance and is investigated below.

13.3.2.4 Effect of the Presence of Salt

From a general point of view, as will be discussed in more detail here, the stability of emulsions is related to the relative interactions of the surfactant with oil and water [40,41]. This property has been used to optimize demulsifier molecules or mixtures for destabilizing emulsions of "regular" crude oils [42]. Indeed, the salinity of water has a strong effect on the interactions of surfactant with water, particularly in the case of ionic surfactants [43–45]: the higher the ionic strength, the lower the interactions with water (and the lower their solubility in water). Therefore, it is expected that, for a given water–oil–surfactant system, changing the brine salinity can produce or destabilize an emulsion. An example is provided in Figure 13.21 where the system contains a naphthenic crude, water, and a demulsifier [42].

It can be seen that a maximum in coalescence rate, i.e., a minimum in emulsion stability, occurs roughly at 60 g/l NaCl for demulsifier I_1. Hence, depending on the starting point, increasing the salinity may stabilize or destabilize an emulsion. Indeed, the effect of multivalent cations is much stronger than monovalent, particularly in the case of carboxylic acids: calcium soaps are known to be sparingly soluble in water. To study the effect of salt, systems presenting an intermediate decantation rate (typically 30% of decanted water after 8 h and 50% after 48 h) were selected.

13.3.2.4.1 Dalia 1

The effect of sodium chloride and calcium chloride has been investigated on the system obtained for $pH_i = 12.1$ ($pH_f = 7.4$) in the absence of salt. Figure 13.22 shows the evolution of the

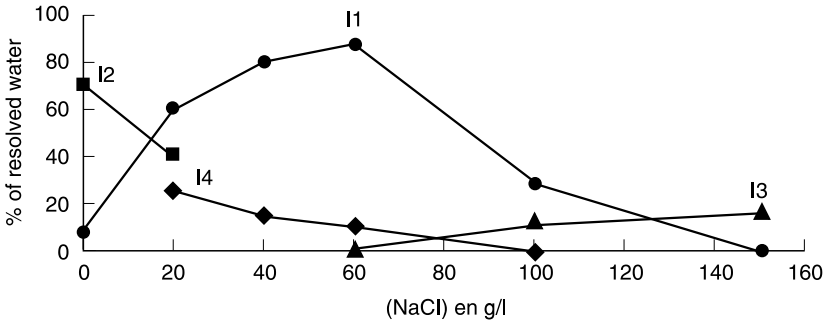

FIGURE 13.21 Effect of brine salinity on the stability of water in crude oil emulsions, in the presence of various demulsifiers (I1 to I4).

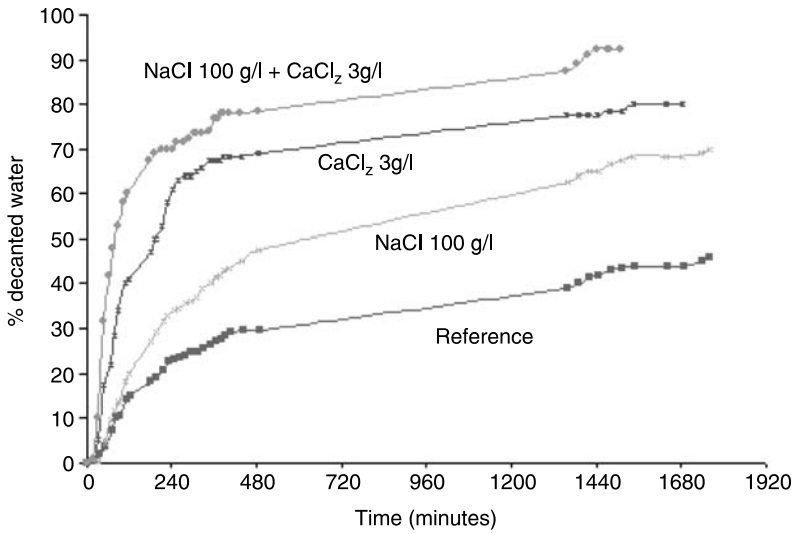

FIGURE 13.22 Effect of sodium and calcium concentrations on the stability of the water in oil (DALIA 1) emulsion. Initial pH = 12.1.

decanted water as a function of time for systems containing various amounts of salt. In all cases the presence of sodium or calcium destabilizes the emulsion.

The destabilizing effect is much more important with calcium than with sodium since only 3 g/l of $CaCl_2$ more than doubles the decantation rate of emulsion after 8 h, while 100 g/l of NaCl are required to increase it by 50%.

It is likely that NaCl destabilizes the emulsion through a modification of the relative interactions of the naphthenates with water and oil, as explained above. In the case of $CaCl_2$, it has been verified that, after phase separation, most of the calcium is located in the crude oil phase. At the same time, the surface tension of the water phase increases [46]. No gel is observed. This shows that the calcium salts of the Dalia 1 naphthenic acids are soluble in the crude. Indeed, in

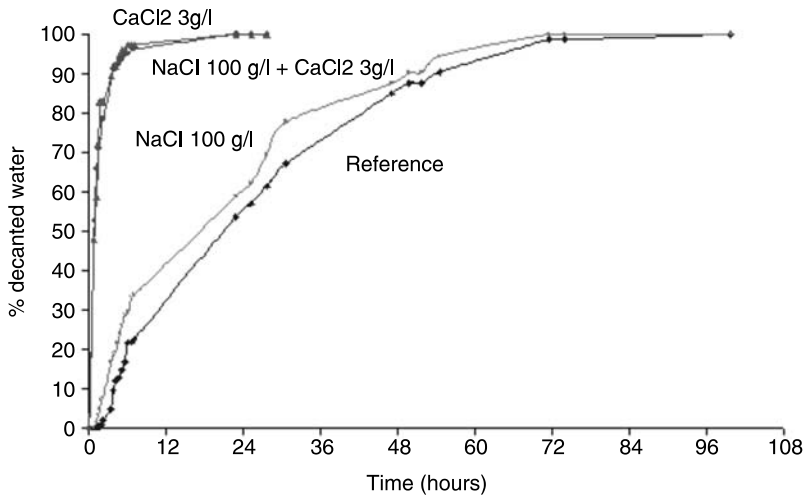

FIGURE 13.23 Effect of sodium and calcium concentrations on the stability of the water in oil (ORQUIDEA) emulsion. Initial pH = 12.5.

that case, adding calcium to the system results in removing some naphthenates from the interface, thus destabilizing the emulsion.

13.3.2.4.2 Orquidea

Figure 13.23 shows for Orquidea the effect of the presence of sodium and calcium on emulsion stability (initial pH: 12.5; final pH: 7.7 when no salt). Contrary to what was observed with Dalia 1 at the same concentration the presence of sodium salt has little effect on emulsion stability, whereas calcium destabilizes strongly the system. Again, no gel is observed in this case.

13.3.2.4.3 Dalia 2

The results are reported in Figure 13.24 (initial pH = 12.5; final pH = 10.5 when no salt). This case is interesting since, as it has been mentioned above, the Dalia 2 crude contains some calcium.

Contrary to what happened with Dalia 1 and Orquidea, the addition of calcium salt has a very small effect on the stability of the emulsion. Some solid gel-like deposit is visible at the interface, similar to that described above for the Dalia 2 behavior (Figure 13.20). The lower pH_f used here (10.5) likely explains why a lower gel concentration, and thus lower emulsion stability, is observed, compared to the systems at $pH_f = 12.5$ in Figure 13.20. Nevertheless, the stabilizing character of the structures formed from Dalia 2 calcium naphthenates is demonstrated.

As regards NaCl, it displays a strong destabilizing effect, even stronger than what was observed with Dalia 1. The surface tension of the aqueous phase extracted from different systems has been measured. The results are reported in Table 13.5. It can be seen that in the presence of NaCl, the surface tension of the aqueous phase is lower than that of the reference system. It shows that the Dalia 2 sodium naphthenates become more surface active at the water–air interface in the presence of NaCl, although they have been measured in lower concentration in the water phase ("salting out" effect). This clearly demonstrates the modification by NaCl of the

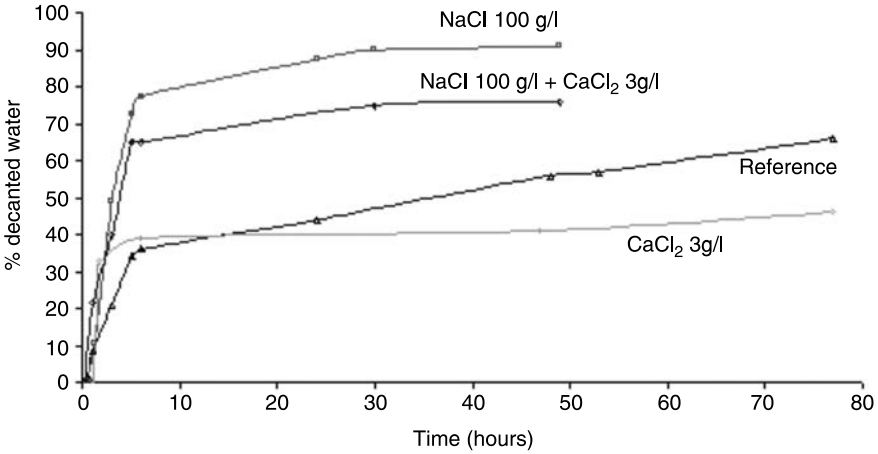

FIGURE 13.24 Effect of sodium and calcium concentrations on the stability of the water in oil (Dalia 2) emulsion. Initial pH = 12.5.

TABLE 13.5
Surface Tension of Aqueous Phase. Dalia 2: pH_i = 12.5; pH_f = 10.5

Salt Concentration (g/l)		Surface Tension (mN/m)	Decanted Water after 8 h (%)
NaCl	$CaCl_2$		
0	0	50	40
100	0	42	90
0	3	51	36
100	3	42	78

interactions of the sodium naphthenates with water. However, this makes them less effective at the water–Dalia 2 interface, because of disequilibrated interactions with oil relative to water.

It is interesting to compare the behavior of the calcium naphthenates of Dalia 1 and Orquidea on the one hand and of Dalia 2 on the other. As it has been shown, the first ones readily dissolve in the oil phase and have no contribution to emulsion stabilization, while the second form structured mesophases (as evidenced by observation under polarized light), displaying viscoelastic behavior and some interfacial activity since they may provide strong emulsion stabilization. Emulsion stabilization by lamellar liquid crystalline phases has been demonstrated in the past [47–49], such mesophases providing interfacial rigidity, thus preventing droplet coalescence.

In Figure 13.25, we propose schematically two types of structural arrangements of the calcium naphthenates which could correspond to the types of above-described behaviors. Type a is a more or less "linear" association of the naphthenates linked by the calcium ion, where the organic chains are solvated by the crude. In type b, the "comb-shape" structure is promoted by strong lateral interactions between the naphthenate molecules and by the structuring presence of water. Indeed, the occurrence of type a or b structure depends heavily on the interactions of the naphthenates

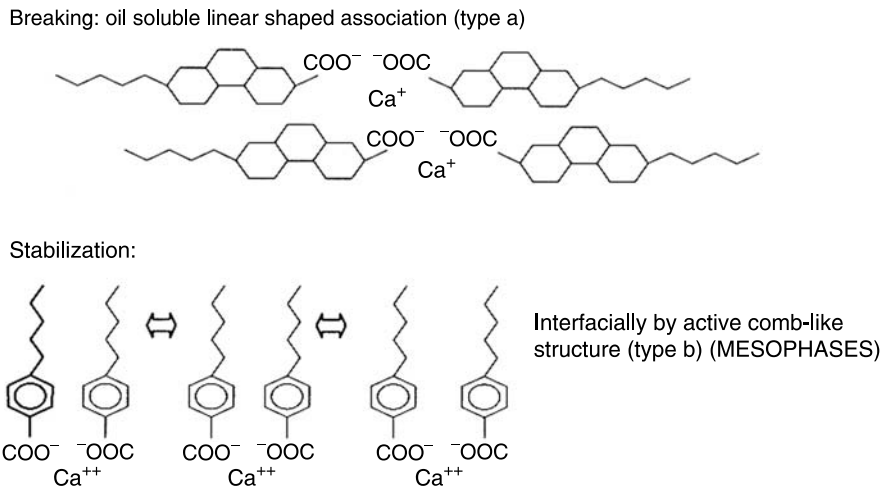

FIGURE 13.25 Hypothetical structures for various types of calcium naphthenates.

with the oil ("solvent quality" of the crude), as well as on the lateral interactions between the naphthenate molecules themselves, which obviously involves steric considerations.

13.4 THEORETICAL ASPECTS

13.4.1 Background to Phase Behavior Modeling

A number of factors contribute to emulsion stabilization, with respect to coalescence, which have to be taken into account for possible modeling. Obviously, the relative interactions of the surface active agents with oil and water are of paramount importance. They are in fact the base of the old Bancroft rule and of the hydrophile–lipophile balance (HLB) concept [50]. More recently, the relationship between microemulsion formulation and emulsion formulation has been established [40]. For optimum microemulsion formulation, it is essential that the interactions of the surfactant with oil and water be equal [44,45]. Under these conditions, at low surfactant concentrations, a third phase containing the surfactant is observed in equilibrium with excess oil and water. Such a system has been found coalescing extremely rapidly, as shown in Figure 13.26.

In that case, the modification of interactions has been achieved through salinity change. At 5 g/l NaCl, phase separation is extremely fast, and, at equilibrium, three phases are observed. On both sides of this system, a maximum in emulsion stability is exhibited corresponding to oil-in-water emulsions at low salinity, where the surfactant interactions with water are higher than those with oil, and to oil-in-water emulsions at high salinity, where it is the reverse. *The general character of this pattern must be recognized: a change in oil type, for example, or in surfactant type, or in temperature, or in any other parameter affecting the interactions at the oil/water interface, will shift the whole diagram towards higher or lower salinities, but the relative positions of the transitions will be maintained.*

This property has been shown to apply also to the case of crude oils, as shown in Figure 13.21 above, and exploited for demulsifier optimization [42], the demulsifier being a surface active molecule able to appropriately modify the interfacial interactions. Indeed, as it has been seen

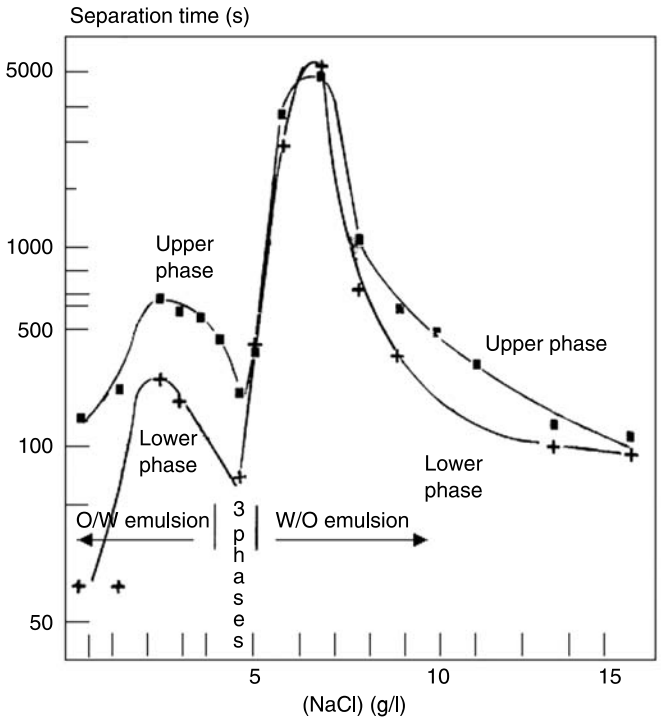

FIGURE 13.26 Time required for half of the considered phase to clear as a function of salinity. Water/hexane = 1; 1.5% petroleum sulfonate (TRS 10-80); 2.5% 2. butanol. Room temperature.

above with the Dalia 2 case, liquid crystalline phases may contribute greatly to the stabilization of emulsions, provided they display an amphiphilic character promoting their adsorption at the oil–water interface.

In the case of organic carboxylic acids, the ionization degree of the molecule, which of course depends on pH, is essential for determining its interaction with water at the water–oil interface. It must be recognized, however, that the acid from RCOOH, where R represents the organic moiety of the molecule, also displays an amphiphilic character. Indeed, this species is much less hydrophilic than the ionized from $RCOO^-$. A change in pH, which changes the ratio of the two species, depending on the pK_a, allows the ratio of the hydrophile to lipophile interactions at the interface to be varied continuously, and thus promote the expected transitions. Alternatively, this can be achieved by mixing the salt and acid species in various ratios, thus determining the pH. This is illustrated in Figure 13.27, which shows the phase behavior of various mixtures of octanoic acid and sodium octanoate in contact with decane and water [45]. Isobutanol has been added to the system to prevent liquid crystalline phase appearing.

For a given salt/acid ratio, for example 75/25 (wt) for which the pH is found to be 7.0, the water salinity (NaCl) is varied and the phase behavior is observed at various surfactant + alcohol (S + A) concentrations. A phase map is thus obtained which comprises four regions: two 2-phase regions on the left and right part of the diagram, a single-phase region (microemulsion regime), and a 3-phase region underneath the previous one, where a surfactant-containing phase is in equilibrium with both excess oil and water phases. High separation rates are observed in

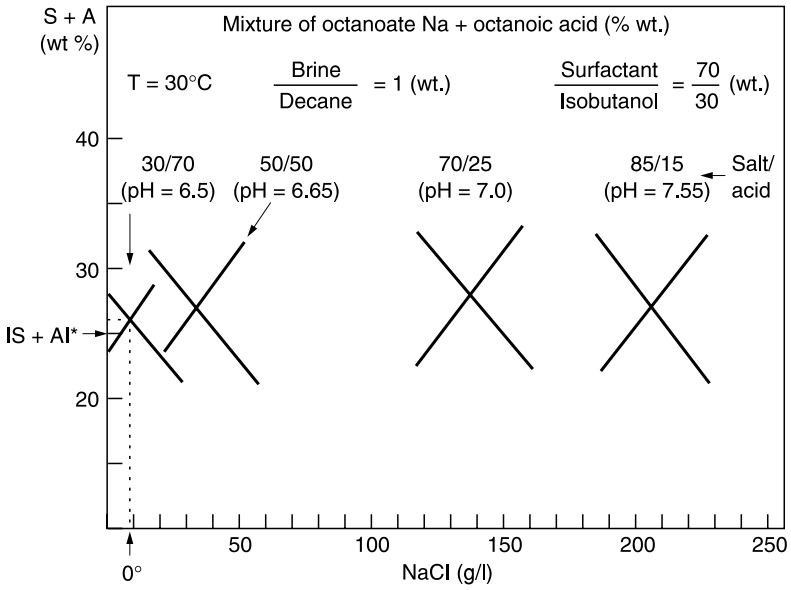

FIGURE 13.27 Sequence of phase maps obtained for various sodium octanoate/octanoic acid ratios when the brine salinity is scanned. For each phase map, the intersection of the straight lines separating regions of different phase behavior defines an "optimal salinity" s*. (After Bourrel M. and Schechter RS. *Microemulsions and Related Systems*: *Formulation, Solvency and Physical Properties*. Surfactant Science Series, Vol 30. Marcel Dekker, New York, 1988.)

this region. The salinity at which the amount of surfactant + alcohol required to reach the single phase region goes through a minimum is called "optimal salinity" s*. The corresponding S + A concentration is noted (S + A)*. At that point, the surfactant (acid + salt forms) interactions with oil and water are equilibrated. A maximum in emulsion stability for water-in-oil emulsions is expected to occur at salinity above s*. It is interesting to note the change in optimal salinity with the sodium octanoate/octanoic acid ratio. Indeed, modifying this ratio does not change the interactions with the oil phase, but changes the interactions with water: increasing the salt/acid ratio entails a strong increase of the interactions with water. To compensate and keep them constant in order to recover the optimal point, the NaCl concentration must be increased since it is well known that the solubility of ionic surfactant in water decreases when the salinity increases ("salting out" effect). This is exactly what is observed in Figure 13.27, demonstrating the interfacial activity of the octanoic acid. This is further emphasized by Figure 13.28 where the optimal salinity has been plotted against pH and compared to the ionization degree α calculated according to:

$$\alpha = \frac{10^{(\mathrm{pH}-\mathrm{pK_a})}}{1 + 10^{(\mathrm{pH}-\mathrm{pK_a})}} \tag{13.1}$$

which in principle is valid only for dilute solutions of weak electrolytes. α is the ratio of ionized molecules to the total number of ionized + non-ionized molecules.

The calculation has been carried out taking $\mathrm{pK_a} = 6.65$, a value which has been experimentally determined from the neutralization curve of the octanoic acid by its sodium salt in the case

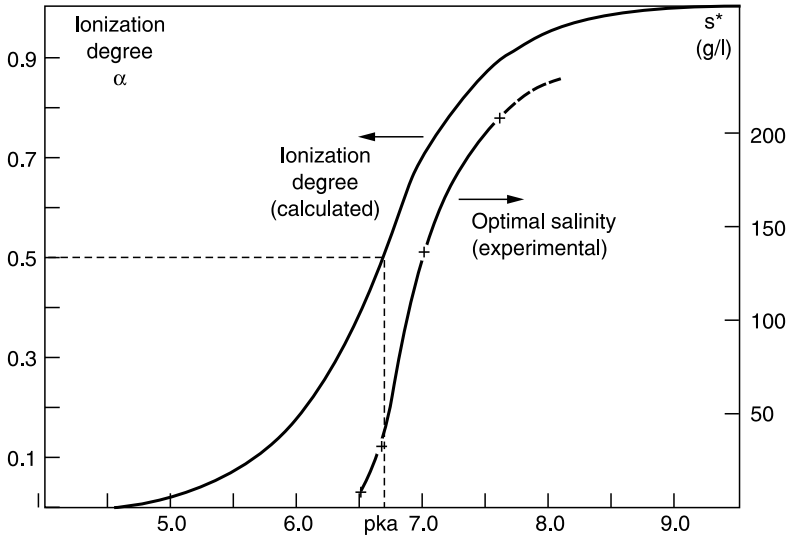

FIGURE 13.28 Correlation between the degree of ionization and optimal salinity s* of Figure 13.27 for carboxylated surfactants. (After Bourrel M. and Schechter RS. *Microemulsions and Related Systems*: *Formulation, Solvency and Physical Properties*. Surfactant Science Series, Vol 30. Marcel Dekker, New York, 1988.)

of brine–decane surfactant + alcohol systems, that is to say in microemulsion systems. It was found to be different from that obtained from highly dilute solutions: $pK_a = 4.89$ at 20 °C. This difference is probably due to the fact that in such highly dilute aqueous solutions, the acid and salt molecules are in monomeric forms, whereas in microemulsions, emulsions, or concentrated aqueous micellar solutions, it is known that the dissociation equilibrium of an electrolyte is affected by the presence of the interface [51,52]. This is even accentuated with brines displaying high ionic strength, due to the double-layer compression effect. In other words, the local pH at the interface is not identical to that measured commonly in the bulk. Additionally, the pK_a of acetic acid has been measured in mixtures of water + ethanol (50/50) and found to be 5.5 instead of 4.7 in pure water. Similarly, for octanoic acid, the pK_a is 6.05 in water–ethanol mixtures, compared to 4.9 in pure water.

Nevertheless, it is interesting to observe in Figure 13.28 that α calculated by Equation 13.1, which is oversimplified, displays the same sigmoidal shape as the optimal salinity when plotted against pH. This gives more support to the conclusion that octanoic acid must be considered as a surfactant when interpreting emulsion phase behavior.

To summarize, the stability with respect to coalescence of water in acidic crude oil emulsion is ruled by the interactions of the naphthenic species *present* at the interface with water, oil, and between themselves. The parameters affecting these interactions are:

- Water side of the interface: pH, salinity (with a dramatic effect of multivalent cations), temperature, naphthenate structure, pK_a
- Oil side of interface: oil type ("solvency quality"), temperature, naphthenate structure, naphthenic acids structure

Indeed, if surface active molecules, such as demulsifiers, corrosion inhibitors etc., are added to the system, they will adsorb at the water–oil interface and modify the above interaction energies, thus affecting the emulsion stability.

It is obvious, as it has been pointed out previously, that the role played by surface active compounds in emulsion stability is determined only by the fraction present at the interface. Species dissolved in the bulk aqueous or organic phase will not participate in emulsion stabilization. From this point of view, it is very useful to treat the interface as a pseudo-phase and to consider the partitioning equilibrium of the surface active species between the oil phase, the water phase, and the interfacial pseudo-phase [52]. This indeed can be described using two partition coefficients of the surfactant: between oil and water phases, and between oil and interface, for example.

This can be a very difficult task, however, when dealing with mixtures of surfactants such as those encountered in commercial products, and, of course, in naphthenic crudes. Good modeling has been carried out for multiphase microemulsion behavior obtained with isooctane, water, and polyethoxylated octylphenols (commercial products presenting the usual Poisson distribution of ethylene oxide number) [53]. This required knowledge of the partition coefficients of each surfactant species. For naphthenic crudes, which comprise distributions of both acidic and salt forms, this does not seem realistic. Furthermore, if the concentrations are not too small, the partition coefficients depend on concentration (non-ideal systems).

Finally, it must be recognized that the area of the interface (i.e., the "volume" of the interfacial pseudophase) depends on the mixing conditions of the system: when dealing with a partly emulsified system, the composition of the resolved water and oil phases may depend on the total area of oil–water interface in the residual emulsion, that is on the initial particle size distribution of the emulsion. Illustrations will be given below. Indeed, for a completely separated system, the interfacial area is small and the phenomenon can be ignored [39].

13.4.2 The Model

The main features observed during the experiments carried out on crude oils are:

- At low initial pH, the final pH is almost constant
- At higher initial pH, the final pH increases dramatically, with a simultaneous stabilization of water in crude oil emulsions

The basic hypothesis explaining the results is that the naphthenic acids of the crude react with the basic in the water phase. They impose the final pH, with respect to their pKa value and concentration in the phases. The sharp increase in final pH at higher initial pH is due to the massive neutralization of the naphthenic acids, and the concomitant emulsion formation due to the surface activity of the dissociated form of the acids. This interpretation can be further detailed by using the simple description presented below.

Let us consider a single naphthenic acid AH, at concentration C_{TAN} initially in the oil phase. Sodium naphthenates A^- could also be present in the oil phase at concentration C_{TBN}. The oil phase (volume V_o) is contacted through vigorous agitation with the water phase (volume V_w), the initial pH of which is fixed by addition of either (H_3O^+,Cl^-) or (Na^+,OH^-) in a known concentration. Naphthenic acid can react when contacted with soda according to:

$$AH + OH^- \leftrightarrows A^- + H_2O$$

Naphthenates can react with H_3O^+ in the water phase according to:

$$A^- + H_3O^+ \leftrightarrows AH + H_2O$$

At equilibrium, we therefore have six unknown concentrations:

- Concentrations in the oil phase: AH_o, A_o^-
- Concentrations in the water phase: AH_w, A_w^-, h, OH^-,

where h is the final proton concentration, i.e., the final equilibrium pH. To calculate these concentrations, we have to simultaneously solve six equations, which are:

- Mass balance:

$$V_o\,(C_{TAN} + C_{TBN}) = V_o\left(AH_o + A_o^-\right) + V_w\left(AH_w + A_w^-\right)$$

- Electroneutrality:

$$V_w\left(A_w^- + OH^-\right) = V_w\,(h + H_i) + V_o\left(C_{TBN} - A_o^-\right)$$

where H_i is either the initial OH^- concentration OH_i or the initial H_3O^+ concentration h_i, the last term on the right side being linked to the number of Na^+ associated to naphthenates transferred from the oil phase to the water phase.

For dissociations in water:

$$K_e = h \cdot OH^-$$

and in acid:

$$K_a = \frac{h \cdot A_w^-}{AH_w}$$

For partitioning we assume a constant partitioning coefficient with respect to concentration and water–oil ratio for both AH and A^-:

$$K_S^{AH} = \frac{AH_o}{AH_w}$$

for AH, and

$$K_S^{A^-} = \frac{A_o^-}{A_w^-}$$

for A^-. From this set of equations, the following equation in the variable h can be derived:

$$\begin{aligned} &h^3 + h^2\left[K_a' + H_i + \frac{V_o}{V_w}C_{TBN}\right] \\ &\quad + h \cdot \left[K_a' \cdot \left(H_i - \frac{V_o}{V_w}C_{TAN}\right) - K_e\right] \\ &\quad - K_a' \cdot K_e = 0 \end{aligned} \tag{13.2}$$

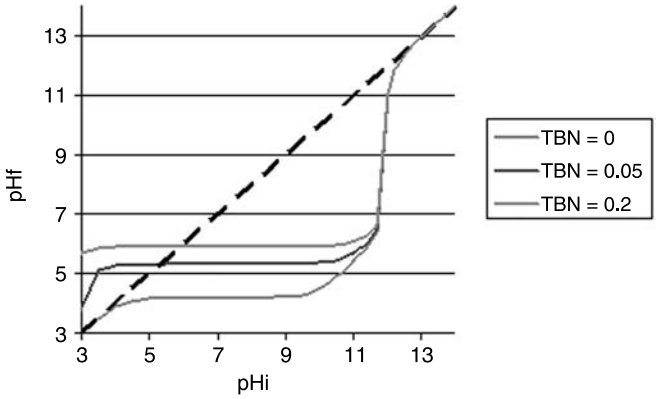

FIGURE 13.29 Calculated final pH as a function of the initial pH for an apparent dissociation constant value of 5.10 to 7 and TAN = 0.5. The TBN value is varied from 0 to 0.2.

where

$$K'_a = \frac{1 + \dfrac{V_o}{V_w} K_s^{A^-}}{1 + \dfrac{V_o}{V_w} K_s^{AH}} \cdot K_a$$

This equation is similar to that obtained in the case of an acid dissolved in a water phase, the dissociation constant of which would be K'_a instead of K_a. The partitioning coefficient of the acid and its conjugate base are therefore incorporated in an apparent dissociation constant of the acid.

Typical calculation results expressed as final pH as a function of the initial pH are shown in Figure 13.29. For this calculation, the apparent dissociation constant K'_a is set to 5×10^{-7}. The TAN of the oil phase is 0.5, and the total base number (TBN), which measures the concentration in sodium naphthenates in the oil phase, is varied from 0 to 0.2. The TBN value has a tremendous effect on the final pH value at low initial pH. Specifically, the final pH can be higher than the initial pH even with a very low and non-detectable concentration of naphthenates in the oil phase. This is important information to correctly interpret experimental curves such as those shown in Figure 13.17.

The physics behind this model is similar to that developed by Havre et al. [39], but has been detailed in order to describe our experimental conditions. Indeed, it has been developed to extract dissociation constant from bottle test experiments, without dosing the acid in the water or oil phase.

It should be pointed out that this modeling does not take account of the fraction of acids at the interface. The main reason for this simplification is that we are considering totally separated systems in which the interfacial area is negligible. The likely micellization of the acids is also discarded, as we are considering diluted systems only.

13.4.3 Application to Model Systems

To test these representations of the complex crude oil/water system, model systems made of carboxylic acid in heptane as an oil phase were used. These systems were studied using the bottle-test procedure described above for the crude oils.

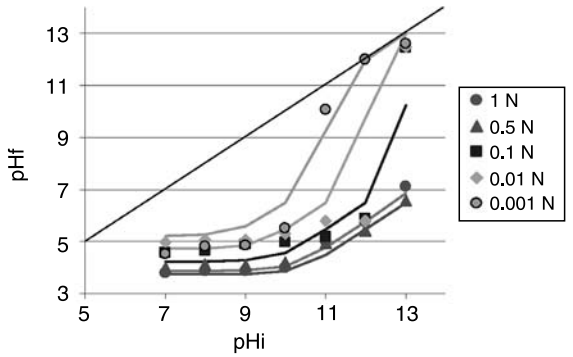

FIGURE 13.30 Final pH vs. initial pH for octanoic acid as a function of initial acid concentration in the oil phase. Solid lines are calculated using Equation 13.2 with pKa = 4.9, $K_S^{AH} = 360$, and $K_S^{A^-} = 0$.

13.4.3.1 Materials and Method

Octanoic acid is used as a model carboxylic acid in this study. Dissolving octanoic acid in heptane produces a model acidic crude, which can be used in bottle-test. Solutions at various concentrations of octanoic acid in heptane were prepared, and placed in contact with aqueous solutions at various initial pH. The pH is fixed by addition of soda in distilled water. The studied acid concentrations were: 1 N, 0.5 N, 0.01 N, and 0.001 N. For each concentration, the initial pH considered was 7, 8, 9, 10, 11, 12, and 13. The water–oil ratio (WOR) in the experiments is 1. The aqueous and oil solutions are prepared in 20 ml tubes that are manually shaken three times. No stable emulsions are observed in these experiments. The final pH is measured on the water phase after 24 h of decantation.

13.4.3.2 Results

Figure 13.30 gives the variation of the measured final pH as a function of the initial pH and the concentration. At a given total concentration, we observe an initial plateau followed by a sudden increase in the final pH. It is seen that the initial plateau depends strongly on the initial concentration of the acid in the oil phase. As expected, the final pH increases when the concentration decreases. The magnitude of the increase at high initial pH also strongly depends on the concentration. When little acid is available to neutralize the soda, the pH increases very rapidly.

Fitting of the data using Equation 13.2 is also reported in Figure 13.30. The generally admitted value of 4.9 is used for the pKa of the octanoic acid, and the partitioning coefficient of the protonated acid is fixed at 360. The partitioning coefficient of the dissociated acid is considered to be 0. The agreement between calculated and experimental values is satisfactory, especially for the higher octanoic acid concentrations.

13.4.4 Application to Crude Oils

13.4.4.1 Determination of Apparent Dissociation Constants

The model described above has been applied successfully to crude oils. Fitting the experimental data at a fixed water/oil ratio can give values of the apparent dissociation constant, which incorporates the partitioning effect, for various crude oils and provides a numerical basis for

TABLE 13.6
Apparent Dissociation Constant Evaluated at a Water Cut of 10% for Various Crude Oils

Crude	pKa′
Heidrun	6.16
Perpetua	7.85
Kuito	8.70
Dalia 1	8.86
Orquidea	9.00
BAP	10.00
Ekoundou	10.45
Dalia 2	13.00

comparison. Values of the apparent dissociation constant determined at a water cut of 10% are reported in Table 13.6. A wide range of values is observed, from a pKa′ value of 6.16 for the Heidrun crude to 13 for the Dalia 2 fluid. The majority of crude tested range from pKa′ = 8 to pKa′ = 9.

13.4.4.2 Relationship to Emulsion Stability

Fitting the final pH values from the bottle test experiments can only give access to the apparent dissociation constant of the crude. To estimate the actual dissociation constant and the partitioning coefficients, more data are needed.

In the case of the Dalia 1 fluid, UV measurements have been performed on the water phase extracted from the bottle tests. It is assumed that UV absorption is mainly sensitive to the dissolved naphthenic acids and naphthenates, thus providing a good indication of their concentration and therefore on the partition coefficient. Consequently, fitting the UV data with the calculated total dissolved acid concentration provides pKa and K_S^{AH} values. First, a fit of the final pH is obtained with an apparent dissociation constant value of pKa′ = 8.86 (Figure 13.31). Then the UV data are used to determine pKa = 7.3 and $K_S^{AH} = 4$ (Figure 13.32). It should be pointed out that the actual TAN value is used in the calculation, and that a small TBN value of 0.001 is introduced to recover a higher final than initial pH value under acidic conditions. The agreement between experimental and calculated values is excellent.

Having determined the dissociation constant and the partition coefficient of the acid, it is possible to calculate the dissociation coefficient of the acid, defined as the percentage of the acid dissociated in the water phase (Equation 13.1).

A good correlation is observed between the dissociation coefficient and non-resolved water fraction in the bottle test experiment, as shown in Figure 13.33. These results suggest that the naphthenates are indeed responsible in this case for the stabilization of the water in crude oil emulsion. It should be pointed out that the stabilization of the water in crude oil emulsion is an interfacial property which is here described by a model considering only bulk phase properties (partitioning and dissociation).

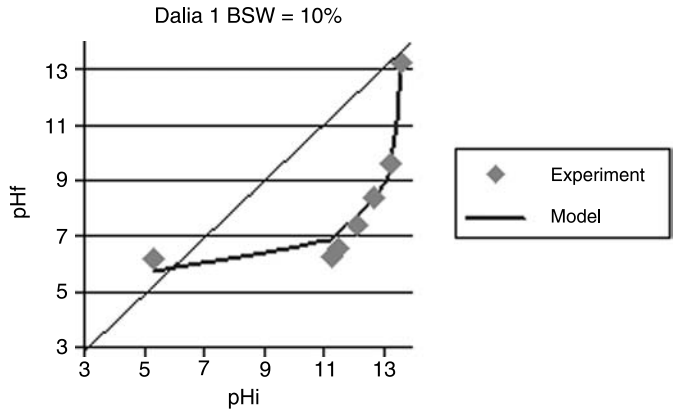

FIGURE 13.31 Final pH vs. initial pH and fitting by the numerical model for Dalia 1. $pKa' = 8.86$.

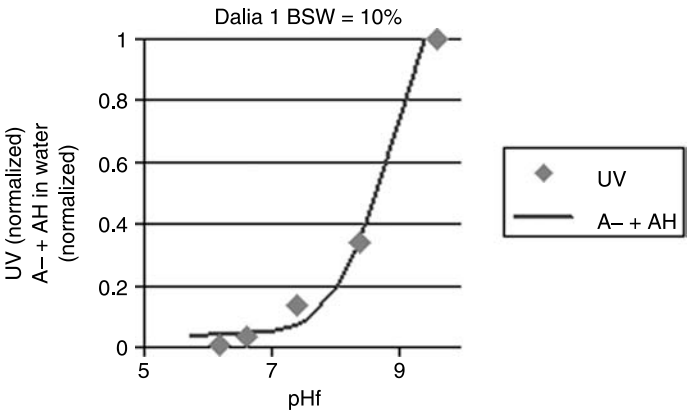

FIGURE 13.32 UV measurements vs. final pH and calculated total acid concentration in water. pKa = 7.3 and $K_S^{AH} = 4$.

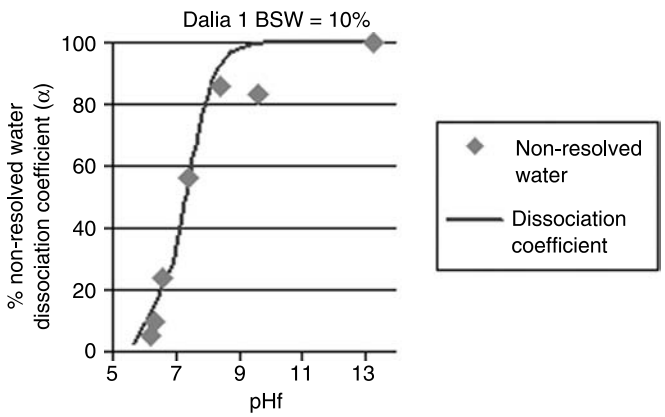

FIGURE 13.33 Non-resolved water and dissociation coefficient vs. final pH for the Dalia 1 case.

13.4.4.3 The Simple Model: Conclusion

The very simple model developed here is shown to be very useful in the interpretation of bottle-test experiments. It can give some insight into the partitioning of the naphthenic acid between the water and oil phases. It should be pointed out that very simplistic hypotheses are used, among which the use of a constant partitioning coefficient. This is probably sufficient only for a limited range of water content and acid concentration, and is the subject of current investigations.

13.5 CONCLUSIONS

The production of acidic crude oils in contact with brines may face several issues, whenever submitted to an increase in pH: coarse emulsion appearance, scale formation, and poor water quality. Predicting such phenomena is a real challenge for oil companies since the design of field equipment depends heavily on their occurrence.

Achieving such a goal generally involves the analytical characterization of the naphthenic acid contained in the crude oil, the laboratory investigation of the phase behavior of crude–brine systems as a function of pH, its modeling, and the confrontation with these findings to the observed field results, whenever available.

The analytical characterization of naphthenic acids has achieved significant progress, especially as a result of the development of mass spectrometry techniques, which provide detailed information on the molecular weight distribution as well as on the functionalities. When applied to field deposits, these techniques have recently allowed the identification of a very heavy tetra-acid which seems to be involved in the occurrence of such deposits. The next challenge is to be able to identify it in crude oils, where its concentration is extremely low. However, these analytical tools cannot determine any physicochemical information, such as pKa, which is of primary relevance for establishing the phase behavior of the system.

On the laboratory scale, this phase behavior seems to be best investigated by using bottle-test experiments carried out over a range of pH. These experiments provide good predictive information, at least regarding the formation of stable emulsions and the quality of the resolved water. Gel-like phases are also obtained, which are much softer than observed on some fields, and may thus be interpreted as the precursors: in field production, there is an accumulation effect over time which is indeed very difficult to reproduce in the laboratory.

Modeling the partitioning of naphthenic acids and their monovalent salts between oil and water works very well on simple model systems, showing that the main characteristics are correctly captured (pKa and partition coefficient). When dealing with acidic crude oils, the results are also satisfactory using as a first approximation a single partition coefficient and a single average pKa value, although it is recognized that more complete data would be required to describe the behavior of such complex systems. For some crudes, for example, it is found that some naphthenic acids do not turn into salt even at high pH, and thus remain in the oil phase. This modeling, however, provides useful guidelines for the investigation of newly discovered acidic oil fields.

Overall, it appears that very significant progress has been achieved in the development of a methodology to tackle possible issues that arise during the production of acidic crude oils. Its validation is on-going by comparing the results with observations carried out on fields presently under production.

ACKNOWLEDGMENTS

The authors wish to express their appreciation to S. Drouilhet, S. Tallet, B. Abbouab, P. Michaud, and H. Dessinet who carried out most of the experiments; to B. Escoffier, A. Goldszal, J.L. Volle, and H.G. Zhou for fruitful discussions; and to the Total management for permission to publish this work.

REFERENCES

1. RF-Rogaland Research Institute, American Chemical Society. Division of Petroleum Chemistry, 43 (1) 142–145 (1998).
2. Tseng-pu Fann. Energy & Fuels, 5 (3) 371–375 (1991).
3. Koike L., Reboucas L., Marsaioli A., Richnow H., Michaelis W. Organic Geochemistry, 18 (6) 851–860 (1992).
4. Robbins W.K. ACS Petrol Chem Div preprint, 43 (1) 137–140 (1998).
5. Nascimento L., Reboucas L., Koike L., Reis F., Soldan A., Cerqueira J., Marsaioli A. Organic Geochemistry, 30 (9) 1175–1191 (1999).
6. Baugh T., Wolf N.O., Mediaas H., Vindstad J.E. Paper presented at the 228th ACS National Meeting, Div. of Pet. Chem., Philadelphia (Aug. 22–26, 2004).
7. Gallup D., Star J. SPE 87471 presented at the 6th International Symposium on Oilfield Scale (May 2004).
8. Brient J.A., Wessner P.J., Doyle M.N. Kirk Othmer Encyclopaedia, Vol.16, 1017–1029.
9. Seifert W., Herz W., Grisebach H., Kirby G. Progress in the Chemistry of Organic Natural Products, 32, 1–49 (1975).
10. Niyazov A.N., Amanov K.B., Trapeznikova V.F., Chirkova B.V. Khim. Geol. Nauuk, 4, 121–123 (1975).
11. Marquez M.L. AIChE Spring National Meeting Session T6005 (March 1999).
12. Vindstad J.E., Bye A.S., Grande K.V., Hustad B.M., Hutvedt E., Nergard B. SPE 80375 presented at the SPE 5th International Symposium on Oilfield Scale, Aberdeen (Jan. 2003).
13. Hurtevent C., Rousseau G., Zhou H.G. Calcium carbonate and naphthenate mixed scale in deep-offshore fields, SPE 68307 presented at the 3rd International Symposium on Oilfield Scale (Jan. 2001).
14. Horvath-Szabo G., Masliyah J.H., Czarnecki J. J. Coll Interf. Sci., 257, 299 (2003).
15. Horvath-Szabo G., Czarnecki J., Masliyah J.H. J. Coll Interf. Sci., 253, 427 (2003).
16. Dyer S.J., Graham G.M., Arnott C. SPE 80395 presented at the 5th International Symposium on Oilfield Scale, Aberdeen (Jan. 2003).
17. Kane R.D., Cayard M.S. Hydrocarbon Processing, 97–103 (Oct. 1999).
18. Hau J.L., Yépez O., Specht M., Lorenzo R. Paper No. 379, Corrosion/99, NACE International, Houston (1999).
19. Naphthenic Acid Corrosion Review Page, Set Laboratories, Internet site: www.setlaboratories.com/nac.htm.
20. Jenkins G.I. J. Inst. Petrol., 51, 501, 313–322 (1965).
21. Meredith W., Kelland S.J., Jones D.M. Organic Geochemistry, 31 (11) 1059–1073 (2000).
22. Jones D.M., Watson J.S., Meredith W., Chen M., Bennett B. Analytical Chemistry, 73, 703–707 (2001).
23. Mediaas H., Grande K.V., Hustad B.M., Rasch A., Rueslatten H.G., Vindstad J.E. SPE No. 80404 presented at the SPE 5th Int. Symp. On Oilfield Scale, Aberdeen (Jan. 2003).
24. Turnbull A., Slavcheva E., Shone B. Corrosion, 54, 922–930 (1998).
25. Corporate Research, Exxon Research and Engineering Co. Book of Abstracts, 215th ACS National Meeting, Dallas, March 29 to April 2 (1998).
26. Messer B., Tarleton B., Beaton M. Paper N° 04634 Corrosion/2004, NACE International, Houston (2004).

27. St. John W.P., Rughani J., Green S.A., McGinnis G.D. J. Chromatography A, 807, 241–251 (1998).
28. Wong D.C.L., van Compernolle R., Nowlin, J.G., O'Neal D.L., Johnson G.M. Chemosphere, 32, 1669–1679 (1996).
29. Hsu C.S., Dechert G.J., Robbins W.K., Fukuda E.K. Energy & Fuels, 14, 217–223 (2000).
30. Miyabayashi K., Suzuki K., Teranishi T., Naito Y., Tsujimoto K., Miyake M. Chem. Lett., 172–173 (2000).
31. Miyabayashi K., Yasuhide N., Miyake M., Tsujimoto K. Eur. J. Mass Spectrom., 6, 251–258 (2000).
32. Zhan D., Fenn J.B. Int. J. Mass Spectrom., 194, 197–208 (2000).
33. Wilm M., Mann M. Anal. Chem., 68, 1–8 (1996).
34. Barrow M.P., McDonnell L.A., Feng X., Walker J., Derrick P. J. Anal. Chem., 75, 860–866 (2003).
35. Seifert W.K., Howells W.G. Anal. Chem., 41 (4), 554–562 (1969).
36. Rousseau G., Zhou H., Hurtevent C. SPE 68307 presented at the 3rd International Symposium on Oilfield Scale, Aberdeen (Jan. 2001).
37. Goldszal A., Hurtevent C., Rousseau G. SPE 74661 presented at the 4th International Symposium on Oilfield Scale; Aberdeen (Jan. 2002).
38. Verzaro F., Bourrel M., Chambu C. "Solubilization in Microemulsions," 5th Int. Symp. On Surf. In Sol., Bordeaux, KL. Mittal ed., 1137–1157 (1984).
39. Havre T.E., Sjöblom J., Vindstad J.E. J. Disp. Sci. Technol., 24 (6), 789–801 (2003).
40. Bourrel M., Graciaa A., Schechter R.S., Wade W.H. J. Coll. Int. Sci., 72, 161 (1979).
41. Salager J.L., Loaiza-Maldonado I., Miñana-Pérez M., Silva F. J. Disp. Sci. Technol., 3, 279–292 (1982).
42. Goldszal A., Bourrel M. Ind. & Eng. Chem. Research, 39 (8), 2716–2727 (2000).
43. Salager J.L., Morgan J.C., Schechter R.S., Wade W.H., Vasquez E. Soc. Pet. Eng. J., 23, 669 (1983).
44. Winsor P.A. "Solvent Properties of Amphiphilic Compounds", Butterworth, London (1954).
45. Bourrel M., Schechter R.S. "Microemulsions and Related Systems: Formulation, Solvency and Physical Properties", Surfactant Science Series, Vol 30, M. Dekker, New York (1988).
46. Goldszal A., Bourrel M., Hurtevent C., Volle J.L. Paper presented at the Spring A.I.Ch.E Meeting New Orleans (March 2002).
47. Friberg S., Mandell L., Larsson M. J. Coll. Int. Sci., 29, 155 (1969).
48. Havre T.E., Sjöblom J. Coll. Surf. A; Phys. Eng. Aspects, 228, 131 (2003).
49. Lucassen J. J. Phys. Chem., 70, 1824 (1966).
50. Griffin W.C. J. Soc. Cosmetic Chem., 1, 311 (1949) ibid. 5, 249 (1954).
51. Stainsby G., Alexander A.E. Trans Faraday Soc., 45, 585 (1949).
52. Biais J., Bothorel P., Clin B., Lalanne P. J. Disp. Sci. Technol., 1, 67 (1981).
53. Graciaa A., Lachaise J., Sayous J.G., Bourrel M., Schechter R.S., Wade W.H. Proceedings of the Second European Symposium on EOR Techniques, Paris, p. 61 (1982).